ADVANCED FUNCTIONAL MATERIALS
www.afm-journal.de

Developments and Challenges in Self-Healing Antifouling Materials

Zhanhua Wang, Luc Scheres, Hesheng Xia, and Han Zuilhof**

Self-healing antifouling materials have gained rapidly increasing interest over the past decade and have been studied and used in a rapidly increasing range of applications. Recent developments and challenges in self-healing antifouling materials are summarized in four sections: first, the different mechanisms for both antifouling and self-healing are briefly discussed. Second, three main categories of self-healing antifouling materials based on surface replenishing and dynamic covalent and noncovalent interactions are discussed, with a focus on the preparation, characterization, and central characteristics of different self-healing antifouling materials. Third, different types of potential applications of self-healing antifouling materials are summarized, such as injectable hydrogels and oil/water separations. Finally, a summary of future development of the field is provided, and a number of critical limitations that are still outstanding are highlighted.

1. Introduction

Deposition of unwanted materials on solid surfaces will cause severe fouling problems, including surface contamination,[1] pipe blocking,[2] metal corrosion,[3] as well as efficiency reduction in microfluidic devices.[4] The fouling material can originate from either living organisms or nonliving substances, and can have a biological,[5] inorganic chemical,[6] or organic chemical origin.[7] Given such detrimental consequences of a wide range of fouling materials and components, there is a rapidly growing interest to understand and reduce fouling. A widely studied bottom-up method to prevent fouling is to design and develop antifouling materials. So far, two rather opposing kinds of antifouling materials have been studied in depth. The first are low-surface energy materials such as silicone[8] and fluorine-containing small molecules or polymers,[9] while the other are high-surface energy materials like PEG[10] and zwitterionic polymers.[11] Next to surface energy variation, these materials can be divided into five categories according to geometrical features and structure: monolayers,[10,12] polymer brushes,[11c,f,13] coatings,[14] gels, and slippery liquid-infused porous surfaces (SLIPS)[15] (**Figure 1**).

The active antifouling mechanism strongly relies on the environment media due to the complicated interactions between fouling agent (foulant), antifouling materials and solvent media. To understand whether a surface will be antifouling toward some foulant adsorption standard thermodynamic considerations is typically sufficient. [In this we will, for reasons of simplicity, ignore specific effects of adsorbed salts or special cases such as weakly bound but still highly ordered solvent layers near the surface.] The free energy of the adsorption process contains an enthalpic component describing the strength of interactions between the foulant, solvent, and surface, and an entropic component denoting the conformation change of the foulant and surface components. Irrespective of the precise details of the adsorption process, it will only occur if $\Delta G_{ads} = \Delta H_{ads} - T\Delta S_{ads} < 0$.

The enthalpic component ΔH_{ads} will dominate in case there are strong interactions between the foulant and surface. Alternatively, when the interaction between foulant and surface is weak, ΔS_{ads} and the temperature will dominate the process of adsorption and/or release.[16] When the antifouling materials have a strong interaction with the environment solvent, the strongly bound solvent layer present at the surface strongly reduces the enthalpic gain of interactions between the surface and foulant, and then ΔH_{ads} in this process is small or even positive. In such situation, the loss of foulant entropy (ΔS_{ads}) dominates during the absorption process, which results in the adsorbed foulant molecules being unstable on the surface. As

Dr. Z. Wang, Prof. H. Xia
State Key Laboratory of Polymer Materials Engineering
Polymer Research Institute
Sichuan University
Chengdu 610065, P. R. China
E-mail: zhwangpoly@scu.edu.cn
Dr. L. Scheres
Surfix B.V.
Bronland 12 B 1, Plus Ultra Building, Wageningen 6708 WH, The Netherlands
Prof. H. Zuilhof
Laboratory of Organic Chemistry
Wageningen University
Stippeneng 4, Wageningen 6708 WE, The Netherlands
E-mail: Han.Zuilhof@wur.nl
Prof. H. Zuilhof
School of Pharmaceutical Sciences and Technology
Tianjin University
92 Weijin Road, Tianjin 300072, P. R. China
Prof. H. Zuilhof
Department of Chemical and Materials Engineering
King Abdulaziz University
Jeddah 21589, Saudi Arabia
The ORCID identification number(s) for the author(s) of this article can be found under https://doi.org/10.1002/adfm.201908098.

DOI: 10.1002/adfm.201908098

a result, they will diffuse back into the solution, resulting in effective antifouling behavior (**Figure 2**A). On the contrary, when the antifouling materials are used in a poor-solvent environment, the antifouling mechanism—in the case of weak foulant-surface interactions—is as follows: the enthalpy obtained (ΔH_{ads}) during the fouling process is small owing to the weak interaction between solvent and antifouling materials. In addition, because of the weak interaction between solvent and antifouling materials, $\Delta S_{ads\text{-}sol}$ will also be very tiny when solvent is replaced by the foulant during the adsorption process. Such small enthalpic gain and minimal loss of order at the surface cannot compensate for the big loss of foulant disorder ($\Delta S_{ads\text{-}foul}$) that accompanies foulant adsorption. Since $\Delta S_{ads\text{-}foul} \gg \Delta S_{ads\text{-}mat}$, any adsorbed foulant will be unstable on the surface and will be easily released into the solution, leading to antifouling (Figure 2B).

No material in this world is perfect, so damage or imperfections of antifouling materials are unavoidable, by either nonideal synthesis, use in relatively harsh environments (caustic, flow) or upon prolonged storage. Any improvement of their service lifetime is of vital importance, both in view of cost and sustainable materials use. Inspired by living organisms that are capable of synthesizing, regenerating, replacing or repairing tissues,[17] a commonly used method to increase the longevity of antifouling materials is the introduction of self-healing properties.[18] Two main working principles are widely utilized to prepare self-healing materials, based on reversible chemical/physical interactions[19] (Figure 2C) or on embedding healing reagents inside the materials matrix[20] (Figure 2D). These can accordingly be classified as intrinsic[21] and extrinsic[22] self-healing materials based on different healing mechanism, and they form the basis of the three categories of self-healing antifouling (further: SHAF) materials that we will discuss in much detail below. We focus here primarily on the molecular events that are responsible for the self-healing process, and on the recovery of structure and mechanical properties after repair. In addition, we do only not look at repair of the features relating to morphology, structure and strength, but aim to reflect in this review the trend that on top of these features aims to restore functions, such as anticorrosion,[23] superamphiphobicity,[24] electrical conduction,[25] antibacterial,[26] and antifouling properties.[27] Among them, SHAF materials attracts great attention in recent years, yielding both a deepened understanding and rapid developments in further applications.[27,28] Several excellent reviews about self-healing[29] or antifouling[29d,30] materials can be found in literature, but the novelty in the current review is the combination of these two facets. We will summarize the recent developments on this topic in this review article.

Generally, we distinguish three main kinds of SHAF systems (**Figure 3**), which focus on the repair of different scales of surface damage. The first category aims to make the material flexible, so that upon small scratches material at both sides of the cut can achieve contact again so as repair the scratch. Such facile and fast repair can prevent the trapping of fouling in the scratch. In addition, repair of the scratch will then also lead to healing of antifouling properties. The second category refers to damage at larger scales, during which part of the material that constitutes the surface is actually lost (e.g., upon abrasion a thin layer is sliced off). Here, flexibility on a molecular scale alone is insuffi-

Zhanhua Wang received his Ph.D. degree in polymer chemistry and physics from Jilin University under the supervision of Prof. Bai Yang in 2011. After that, he worked as a postdoctoral fellow with Prof. Marek Urban in the University of Southern Mississippi and Clemson University. He then moved to Wageningen University as a postdoctoral researcher and worked with Prof. Han Zuilhof until 2016. Presently, he is an associate professor at the Polymer Research Institute of Sichuan University. His current scientific interests are focused on stimuli-responsive polymer composite photonic materials, bioinspired self-healing and antifouling coatings, and self-healing and 3D printing polymer or polymer composite materials.

Hesheng Xia is a Professor and Deputy Director of State Key Lab of Polymer Materials Engineering (China), Sichuan University. He received his bachelor's and master's degrees from Northeastern University in 1994 and 1997, respectively, and Ph.D. degree in materials science from Sichuan University under the supervision of Prof. Qi Wang in 2001. In 2003–2005, he worked as a Research Associate in the Department of Materials, Loughborough University, UK. His main research interests include graphene/carbon nanotube polymer composites, self-healing polymer materials, dynamic polymer materials for 3D printing, and ultrasound mechanochemistry.

Han Zuilhof is the Chair of Organic Chemistry at Wageningen University (Wageningen, The Netherlands), Perennial Distinguished Guest Professor of Molecular Science at Tianjin University (Tianjin, China), and Distinguished Adjunct Professor of Materials Chemistry at the King Abdulaziz University (Jeddah, Saudi Arabia). He is a cofounder of Surfix B.V. (with Luc Scheres). His research interests focus on surface-bound organic chemistry, and the accompanying analytical chemistry to properly characterize that, and on novel supramolecular materials.

cient, and full reformation of the surface by surface restructuring is required. Rather than focusing on fast repair, mechanical strength is prioritized and—given that material loss occurred—the surface functions. The third kind relates to antifouling coatings that try to combine these features, i.e., both repair of nano/microscratches and replenish surface properties including antifouling characteristics. Formation of materials that fall into this third, most stringent category is linked to the balance between enough flexibility to allow molecular mobility on one hand, and sufficient structural strength to withstand abrasion and surface restructuring on the other hand. Since it is difficult to predict the "where, when, and degree" of material damage during the lifetime of a material, new kinds of antifouling materials that integrate a self-healing structure, mechanical strength and optimal surface properties are highly sought after.

Figure 4 schematically illustrates the stepwise process of preparation and characterization of SHAF materials. During the preparation process, the moieties responsible for SHAF characteristics are introduced into the composite systems. They can either be covalently bound to or dispersed into the network matrix. Their ratio and position in the system needs to be precisely controlled to achieve both excellent self-healing and antifouling properties. In some systems, one chemical entity is responsible for both self-healing and antifouling properties, while in other systems different groups need to be combined together to endow this dual functionality. Even more precision is required in the characterization of the damage: minor, and often highly localized fractures and dislocations not present in freshly prepared material, might yield both loss of mechanical strength and antifouling characteristics in damaged materials. Both facets need to be addressed in detail, so as to see in the repaired phase to which degree both strength and antifouling have been regained.

In the following we will first discuss three main classes of SHAF materials: materials based on surface replenishing (Section 2.1), materials based on dynamic covalent or noncovalent interactions that repair structural/shape damage (Section 2.2), and materials that combine both these facets (Section 2.3). Subsequently a range of potential applications is summarized (Section 3), after which we present a brief outlook onto this field.

2. Three Main Categories of Self-Healing Antifouling Materials

2.1. Repair by Surface Self-Replenishing (Category I)

2.1.1. Surface Regeneration of Low-Surface-Energy Materials in Air

Compounds with a low surface energy, such as fluorinated molecules or silicones, are widely used to prepare antifouling materials. These materials naturally locate at the air interfaces to minimize the surface energy of the system and will affect hydrophobicity and lead to very good antifouling properties. Damage of such surfaces will remove these low-surface energy components, with concomitant loss of the SHAF functionality. Regeneration of the surface chemical composition can be achieved by promoting the 1) reorientation, 2) self-segregation/migration, or 3) desorption of low-surface energy components to move toward the new air interfaces to reduce the increased surface energy created by damage. These components should be incorporated into the material beforehand via deposition, adsorption, or chemical grafting reactions with the bulk components.

In the last decade, an autonomous and intrinsic self-healing process, named as self-replenishing,[31] was reported to regenerate the surface wettability of hydrophobic polymer coatings that was lost by wear or shallow scratches at the surface. This behavior was mainly attributed to the reorganization of the dangling polymer segments that are covalently bound onto the crosslinked polymer network toward the damage surface. This movement of the polymer chains was driven by the energy difference between the damaged area and the original materials. The proof of principle of this idea was reported by Esteves, De With and co-workers for hydrophobic polymer films that are composed of crosslinked polyurethanes containing perfluoroalkyl dangling chains chemically bonded (on one side) into the crosslinked network (**Figure 5**A). The surface was damaged by purposely removing a few micrometers of the top layer. The complete recovery of the initial hydrophobicity was confirmed by water contact angle (CA) measurements and from the recovery of F/C atomic ratios determined by X-ray photoelectron spectroscopy (XPS). Depositing or grafting fluorinated materials onto a micro- or nanostructured substrate will lead to a superhydrophobic surface,[32] which will possess better antifouling properties than modifications onto flat surfaces.[33] In their subsequent work, they deposited these polyurethanes coatings onto SiO_2 nanoparticles, and used these to prepare self-replenishing superhydrophobic surfaces (Figure 5B).[34] These surfaces remained superhydrophobic even after 500 damage-repair cycles, while XPS analyses showed that this repeated damaging-repair process yielded only a slight increase in the F/C atomic ratio in the top 10 nm compared to the original surface. These results indicate a reorganization of the dangling fluoropolymer segments moving toward the new air interfaces to regenerate the original surface characteristics. These self-replenishing composite systems were further analyzed by coarse-grain simulation, which can provide the distribution profile of the dangling chains. The results thereof show that the minimum thickness to achieve such high-quality self-replenishing is about 30 nm.[35] Zhang's group reported analogous work in which a branched thiol-ene click-derived fluoroalkyl siloxane is introduced to obtain a self-healing superhydrophobic 3D sol–gel network with dangling fluoroalkyl chains with the aim to coat fabric. The coated fabric was highly durable, and was able to repair itself even 1000 cycles of abrasion under 45 kPa or upon treatment with strong acid/base, UV irradiation or heating. This restoration of its excellent liquid-repellent SHAF properties using the mobility of long dangling perfluoroalkyl arms.[36]

Li et al. developed a self-healing superhydrophobic coating by depositing fluoroalkyl silanes onto a porous polyelectrolyte complex, which was fabricated through alternatively deposition of poly(allylamine hydrochloride) and sulfonated poly(ether ether ketone). This coating displayed self-healing properties due to the transfer to the (damaged) surface and subsequent reaction of fluoroalkyl silane that were stored more deeply in coating layer (**Figure 6**A).[37] Upon damage by an O_2 plasma this material restores its superhydrophobicity after being cured at room

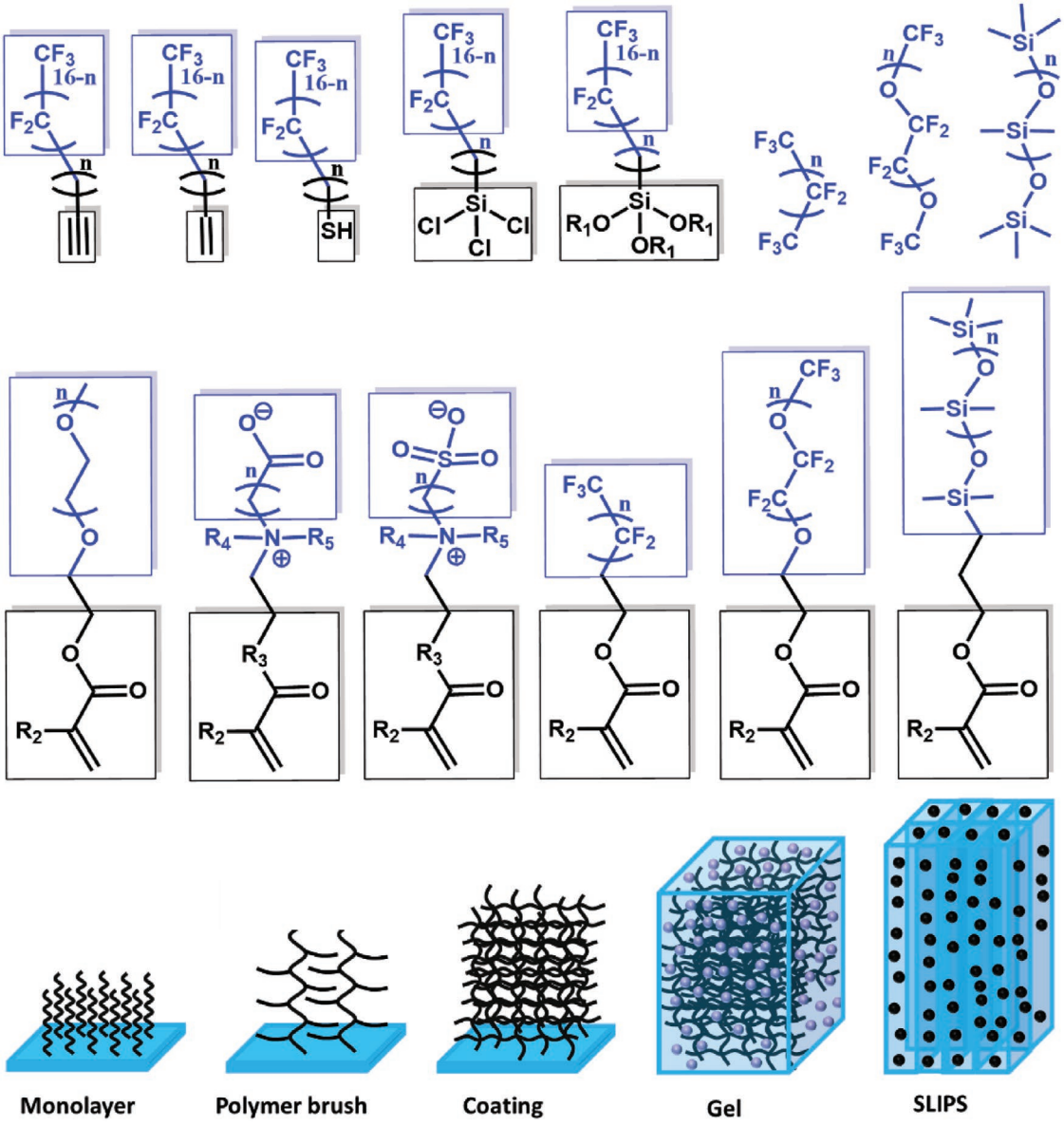

Figure 1. Molecular structures of the typical compounds used for antifouling materials, and schematic illustration of different kinds of materials fabricated based on these compounds. R_1–R_5: typical alkyl moieties.

temperature with 40% humidity for 4 h, to a CA of 158° and a sliding angle of less than 28° (Figure 6B). The regeneration of the superhydrophobicity indicates that the damaged coating is repaired with the fluoroalkyl chains back on top. As shown in Figure 6B, this etching–healing process can be repeated many times without decreasing the superhydrophobicity of the healed coating. These superhydrophobic coatings can be composed of a large number of reacted fluoroalkyl silane moieties as healing agents, explaining such repeatable easy recovery. In addition, once the primary top layer of fluoroalkyl silane molecules are decomposed or scratches are made on the superhydrophobic coating, the poly(acrylic acid) (PAA)-bound fluoroalkyl chains that are present in subsurface layers can slowly but steadily move toward the surface under a slightly humid environment, thereby thus partially mixing the PAA and poly(ether ether ketone) layers, to heal the superhydrophobicity. Since then, extensive studies have been reported about self-healing superhydrophobic surfaces,[38] which enabled long-lived superhydrophobic surfaces and long-term antifouling materials.[39]

The antifouling properties on the nanostructured surfaces might be further improved by achieving superamphiphobicity. Wang et al. developed the first repairable superamphiphobic coating by depositing a fluorinated-decyl polyhedral oligomeric silsesquioxane and a fluoroalkyl silane onto a fabric substrate. This superhydrophobic coating became superamphiphilic, as manifested by the decrease of CA of 0° to both water and oil, upon severe damage by external stimuli such as chemicals, plasma or strong alkali. Facile thermal treatment at 135 °C then regenerated the original superamphiphobicity.[40] Since then, a considerable number of papers have been devoted to

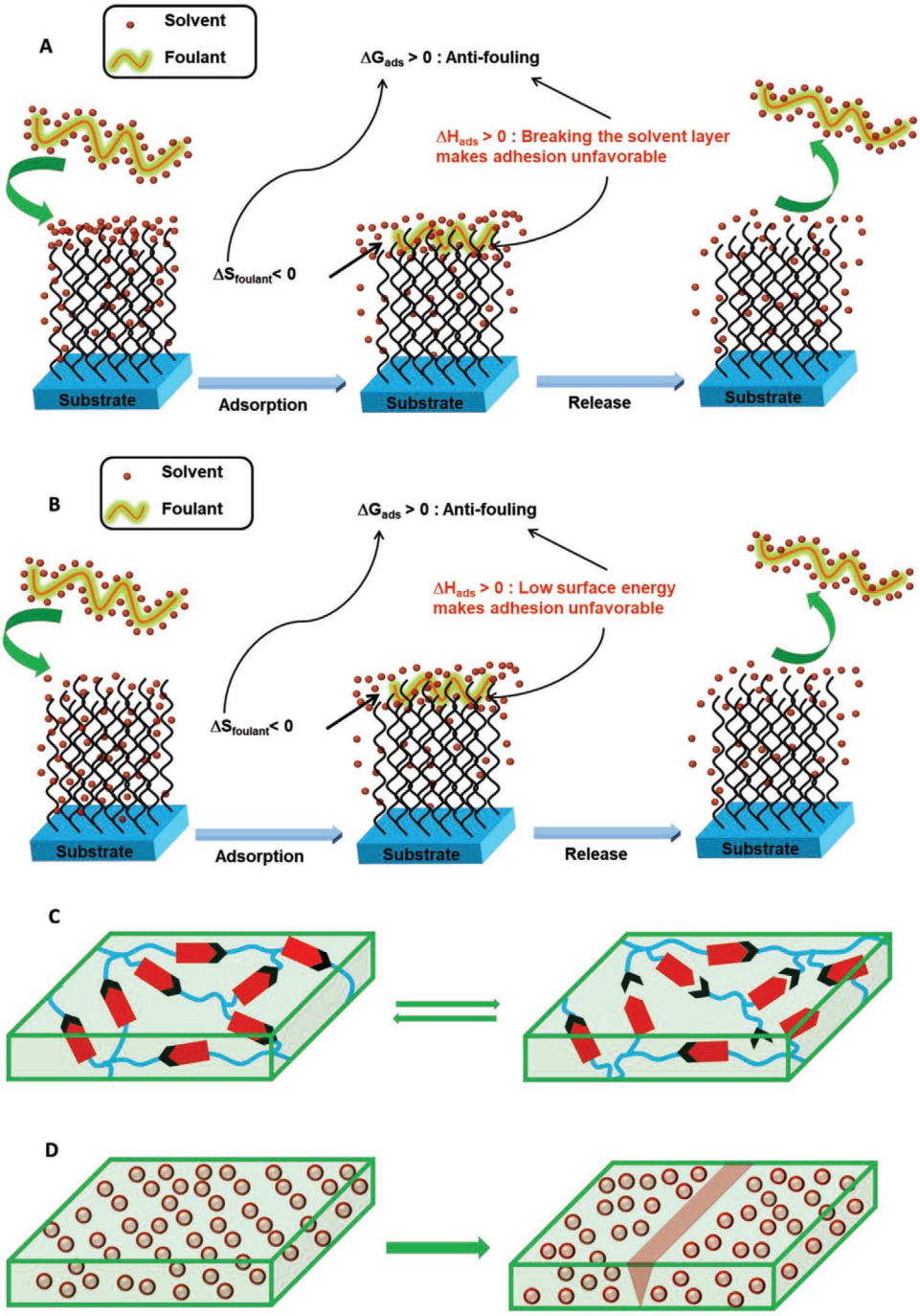

Figure 2. Schematic illustration of the antifouling mechanism induced by high-surface-energy material A) and low-surface-energy materials B). Self-healing mechanisms hinging on dynamic covalent or noncovalent bonds C) and (irreversible) release of encapsulated healing reagents D).

the fabrication of self-healing superamphiphobic materials. A robust, superamphiphobic fabric was fabricated by covering the fabric surface with a mixture of a commonly used, commercially available fluoro-containing polymer, poly(vinylidene fluoride-hexafluoropropylene) (PVDF-HFP), a fluoroalkyl silane (FAS) and silica nanoparticles that were modified by FAS (Figure 6C).[24a] The coated fabric displayed superamphiphobicity as manifested by a CA of > 160° to both water and oil. In order to study the self-healing superamphiphobicity, the coatings were damaged by plasma or strong base, effecting the coating to become amphiphilic through the introduction of oxygen-containing groups, yielding very low contact angles to water, soybean oil and hexadecane.[41] Heating the plasma-treated fabric at 130 °C for 5 min fully restored the superamphiphobicity (Figure 6D). Figure 6E shows the change of CA over the first 10 plasma-heat repair cycles. With more damage-repair cycles (up to 100; see Figure 6F), the CA reduced slightly, but it was still in the superhydrophobic range. In their subsequent

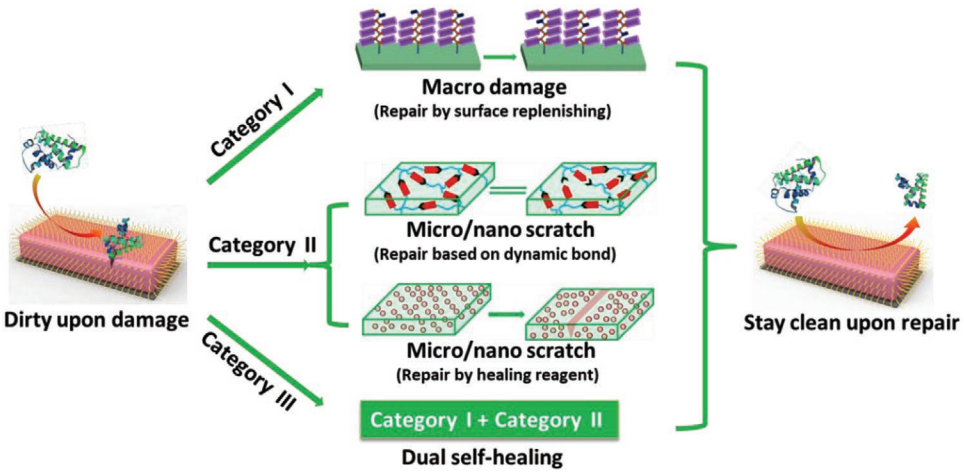

Figure 3. Schematic illustration of the three main kinds of SHAF materials. Category III is obviously the most demanding.

work, these authors utilized amphiphobic nanoparticles, fluorinated alkyl silane, and fluorocarbon surfactants to prepare a stable dispersion in water that is suited for fabricating stable superamphiphobic surfaces on various solid substrates, such as fabrics, sponge, wood, glass as well as metal.[24b] After being covered by this ternary coating system, these materials displayed superamphiphobicity with low contact angle hysteresis. The coating can withstand abrasion, boiling water, and high and low pH treatments, which is hypothesized to be due to previously unreacted fluorinated alkyl silane molecules that will move to the surface upon damage and react there.

Many studies on superamphiphobicity have been reported,[42] often with fabric as substrate, which is partially linked to the roughness on nano- and micrometer scale that is inherent to the fibers present in fabric, which facilitates superhydrophobic characteristics.[43] Hierarchical roughness on these scales can be enhanced by coating the fabric surface with nanoparticles, which will finally contribute to the superamphiphobic properties. While superhydrophobic materials have recently been prepared using fluorine-free coatings,[44] all superamphiphobic coatings reported involve fluorinated compounds. Now the use of fluoro alkyl chains with only a few fluorine atoms is environmentally acceptable, but poly fluoroalkyl chains (such as C_8F_{17}) display significant bioaccumulation and toxicity. Their use in the examples above should therefore be seen as illustrating proof of principle, but a search for short-chain fluorinated (such as CF_3 or CH_2F) alkyl substances or even fluorine-free moieties for making superamphiphobic fabrics should be a central focus in future research as self-healing without environmental sustainability is not worth going after.

Although many self-healing superhydrophobic or superamphiphobic materials have been developed, the hydrolytic stability of the fluorinated materials involved is typically low. In addition, fouling was typically only studied toward low-molecular weight compounds. In order to overcome both these challenges in one study, Wang and Zuilhof extended this strategy to prepare SHAF fluoropolymer brushes through covalent bounding.[13a] A 75 nm fluoropolymer [poly(2-perfluorooctylethyl methacrylate)] (PMAF17) brush was grown onto a Si(111) surface by surface-initiated atom transfer radical polymerization (SI-ATRP). This highly hydrophobic polymer brush withstood fouling from a large series of polymers in different organic media. Upon damage in harsh environments (high/low pH or UV), both the surface wetting and the antifouling properties of the polymer brush could be repaired by a simple heat treatment, and this damage-repair process could be repeated many times. This process was rationalized to occur via the molecular reorganization of the fluorinated tails at the surface–air interface (**Figure 7**B,C), which was confirmed by XPS results: the fraction of C atoms connected to fluorine decreases from 57% initially to 49% after alkaline damage, suggesting partial loss of fluorinated tails due to the ester group hydrolysis in basic environment. This ratio is almost fully recovered upon heating, which is interpreted to be due to the following process: first, carboxylic acid groups are formed at the top of the layer during the hydrolysis/oxidation process. At elevated temperatures, above the T_g of the polymer brush (40 °C), polymer segments display a high enough mobility to reorganize itself and reform an optimized surface driven by the low surface energy of the fluorinated materials.

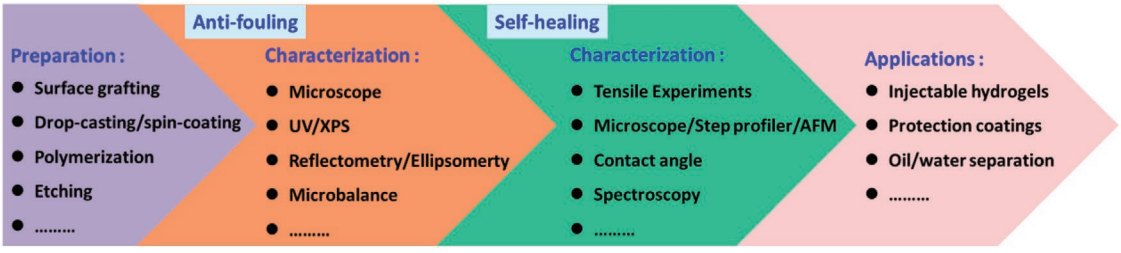

Figure 4. Schematic illustration of the stepwise process of preparation and characterization of SHAF materials.

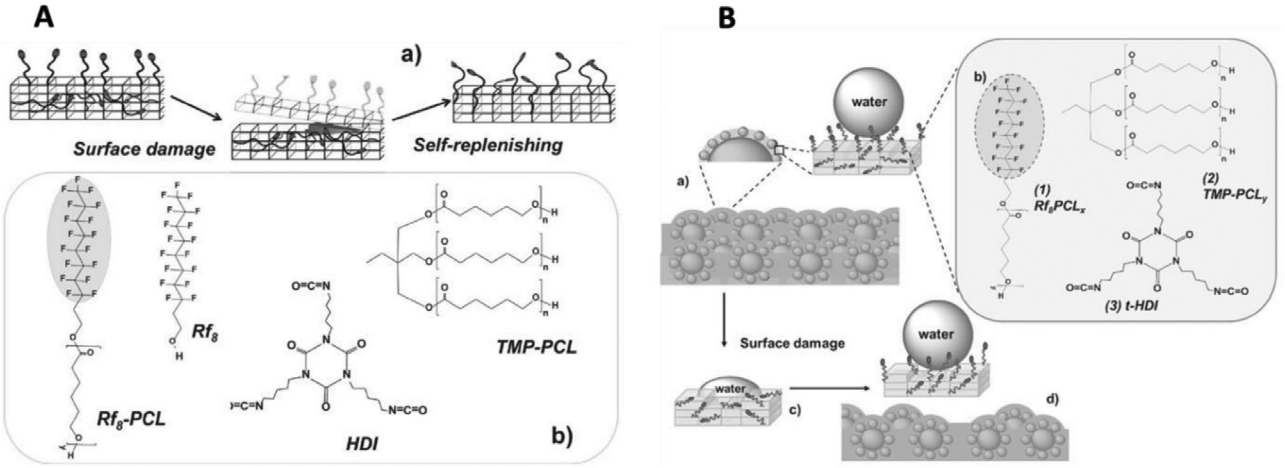

Figure 5. A) Scheme of the self-replenishing mechanism and chemical structures of the components of self-replenishing coatings. Reproduced with permission.[31] Copyright 2012, Wiley-VCH. B) Schematic representation of self-replenishing of surface-structured superhydrophobic coatings. Reproduced with permission.[34] Copyright 2014, Wiley-VCH.

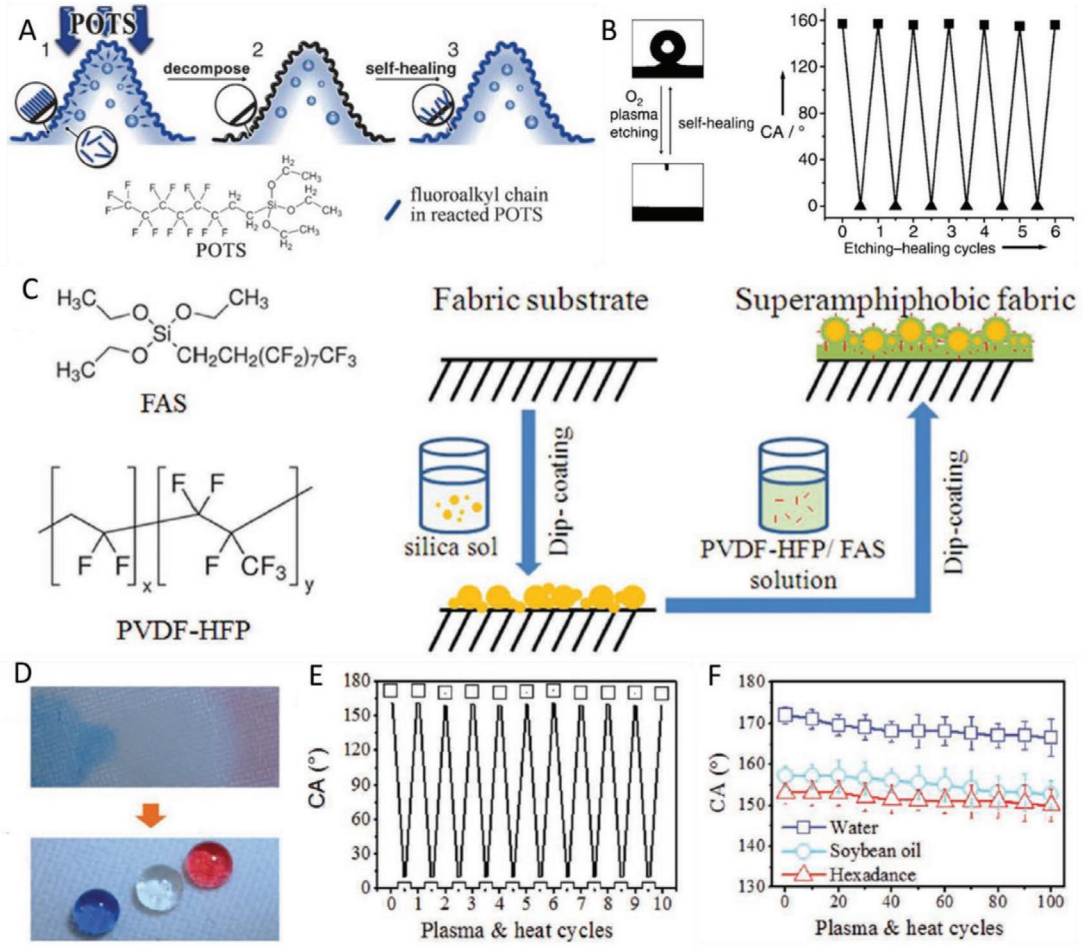

Figure 6. A) Mechanism of self-healing superhydrophobic coatings via secondary reaction of embedded silane molecules. B) Repeatable damage–repair cycles between superhydrophobic (top) and superhydrophilic (bottom) states of the coating in (A) upon O_2 plasma etching and self-healing, and concomitant contact angle changes. Reproduced with permission.[37] Copyright 2010, Wiley-VCH. C) Chemical structure of FAS and PVDF-HFP and coating procedure for superamphiphobic fabrics. D) Photographs of colored liquids (water (blue), hexadecane (red) and soybean oil (clear)) on the coated fabric after the first plasma treatment (top) and after 100 cycles of plasma and heat repair treatments (bottom), and concomitant water CA changes in the first 10 damage–repair cycles E) and prolonged CA changes with several fluids up to 100 damage–repair cycles. Reproduced with permission.[24a] Copyright 2013, Wiley-VCH.

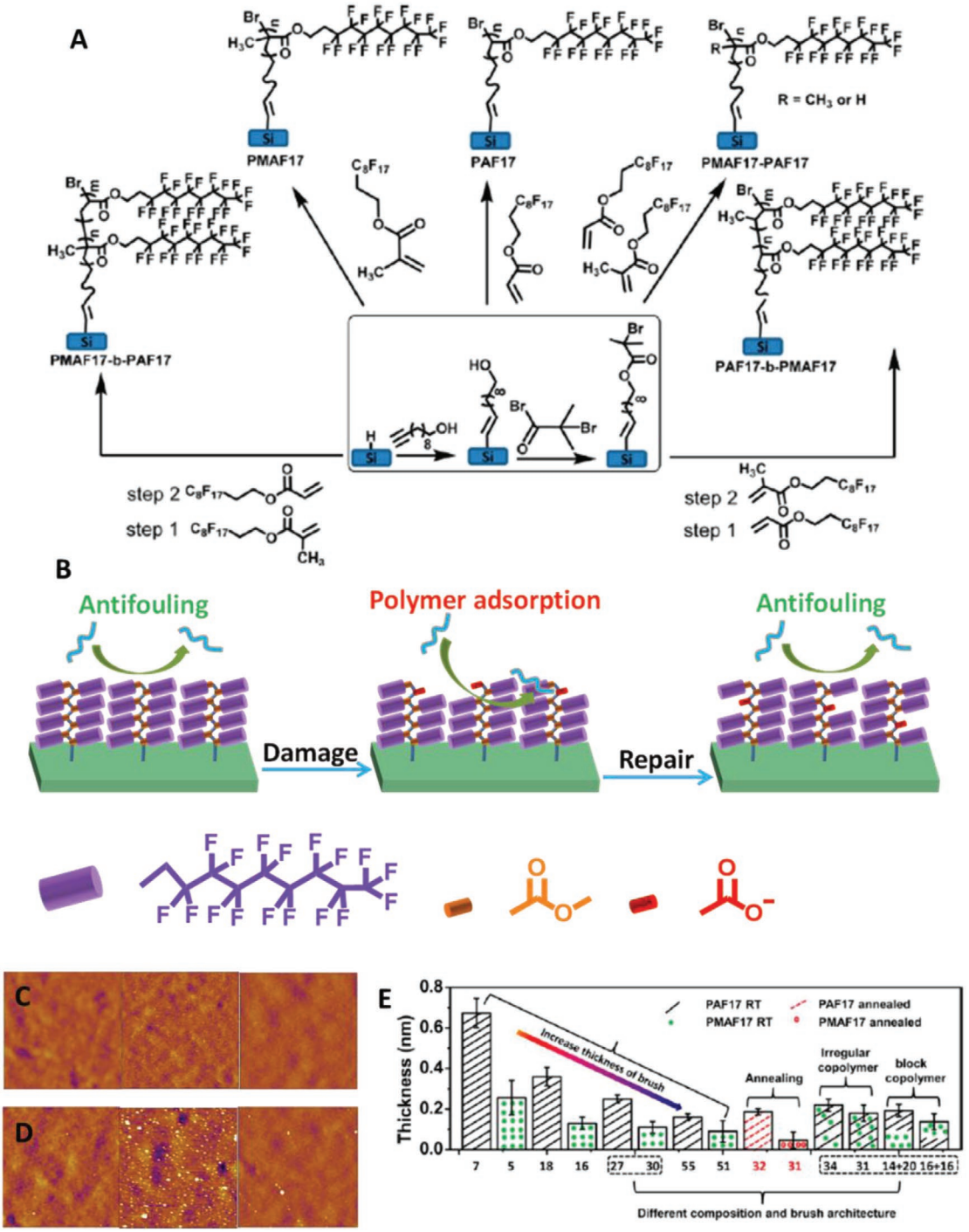

Figure 7. A) Schematic representation of surface functionalization, initiator immobilization, and preparation of the fluoropolymer brushes with different architectures. B) Schematic illustration of the antifouling behavior of the original, damaged, and repaired PMAF17 brush upon immersion into a polymer solution. C) AFM image of the original, damaged, and repaired PMAF17 brush. D) AFM images of the original, damaged, and repaired PMAF17 brushes after immersion into PS–toluene solution for 12 h. Reproduced with permission.[13a] Copyright 2016, Royal Society of Chemistry. E) Degree of fouling (derived from XPS data on thickness increases upon immersion in fouling polystyrene–toluene solution for 12 h) for polymer brushes with different thicknesses and molecular architectures after dipping. Reproduced with permission.[13b] Copyright 2016, American Chemical Society.

This induces undamaged fluorinated tails present in the subsurface layer to migrate toward the surface, and thus bury the recently formed polar moieties, and thereby repair the hydrophobicity and antifouling characteristics. The freshly prepared brush displays excellent antifouling, while heavy fouling indeed happens on surfaces that were damaged in a solution with pH 11 for 24 h. In contrast, heating of damaged surfaces at 120 °C for 2 h followed by immersion of the resulting repaired

surface into a fouling polymer solution yielded a fully non-fouled surface, as no remaining fouling polymer was observed after rinsing, illustrating full repair of the PMAF17 brush with respect to its antifouling characteristics (Figure 7D).

In a later study by the same authors, the influence of parameters such as brush composition, architecture, and post-treatment on the SHAF properties was also studied. A range of fluoropolymer brushes (Figure 7A) with different compositions, thicknesses (30–100 nm) and architectures (homopolymer and block copolymer and random copolymer brushes) was grafted onto silicon surfaces via SI-ATRP of 2-perfluorooctylethyl methacrylate (MAF17) and 2-perfluorooctylethyl acrylate (AF17).[13b] These brushes also displayed excellent antifouling property against organic polymers, which further increased (i.e., less fouling) with increased polymer brush thickness. For the polymer brush with different architectures, the homopolymer brush PMAF17 displayed the best antifouling properties. Annealing of the fluoropolymer brush will induce the reorganization of the surface composition to present more fluoroalkyl chains at the surface, which further increases the hydrophobicity and antifouling properties (Figure 7E). A detailed analysis of the process of adhesion and subsequent antifouling mechanisms outlined the balance of interactions between the brush, fouling polymer and solvent. In case there is a strong attraction of the foulant toward the surface, the adsorption is driven by an enthalpic gain. In the case of a weak interaction between polymer and surface, i.e., with a small enthalpy of adsorption, as is the case for many organic polymers onto this brush, and when the interactions between the solvent (here toluene) and the surface are also weak, then entropic contributions dominate. This is, for example, obvious from changes that occur between the PMAF17 and PAF17 brushes (R = H or CH_3)—which are electronically highly similar, just different T_g and mobility and between brushes of different thickness. In conclusion, for fluoropolymer brushes with a constant degree of fluorination, brushes with higher T_g and thickness display the best antifouling properties, as they effect the largest loss of entropy and smallest enthalpy gain upon adsorption.

In order to further improve the antifouling properties, the same group extended their study to investigate the SHAF characteristics of nanostructured PMAF17 fluoropolymer brushes.[13c] The results displayed that this is possible by grafting this fluorinated polymer brush onto nanostructured silicon surfaces, which were prepared by etching silicon in a silver nitrate-containing HF solution (**Figure 8**A). The reason behind this improvement is the transition from hydrophobicity to superhydrophobicity, due to the surface roughness increase from the nanostructure. Brushes damaged by air plasma could be fully repaired by heating at 120 °C: the static water CA decreased from 152° to 135° upon plasma etching, but then fully recovers to the original value after a 30 min thermal treatment (Figure 8B), and this cycle could be repeated at least five times (Figure 8C). Compared with the self-healing process of the flat PMAF17 brush, this nanostructured PMAF17 brush shows a shorter repair time (30 vs 120 min), which was attributed to a larger interbrush space on the nanostructured surface, allowing an easier reorganization of the brush segments upon heating the sample, leading to faster self-healing. In addition, the increased space is also favorable for segments buried more deeply in the brush to move to the surface and replace any damaged moieties there. For damaged nanostructured fluoropolymer brushes, strong protein adsorption was observed, as confirmed by XPS and CA results. Some protein fouling happened on the repaired brushes, but this was only ≈10% of that of the damaged surfaces, which means that the antifouling properties were recovered quite well after self-healing. Of crucial importance to the overall topic of this review, after five damage–repair cycles, the fouling induced by protein adsorption was about 50% of that of damaged PMAF17 brushes (Figure 8D), even though the CA values fully recovered. Therefore, we propose that for fluorinated/low-surface energy surfaces that display good CA recovery the fouling by proteins is studied, as this is evidently a more stringent, yet easy-to-use test for the full recovery of surfaces labeled as self-healed. Except for fluorinated materials, silicone-based materials or long alkyl chain-containing materials can also be used for fabricating SHAF materials. For example, PDMS-grafted wood surfaces can display excellent underwater durability, antifouling, antismudge, and self-healing properties due to the flexible backbone, low T_g and surface energy of PDMS.[45] Fabrics modified by polydopamine@octadecylamine nanocapsules also displayed robust and healable antifouling, due to the fact that the damage induced the migration of octadecylamine molecules to the surface.[46]

The time needed for such self-healing processes highly depends on the segment flexibility and temperature. When the T_g of the materials is higher than room temperature, thermal treatment is required to melt the frozen chain, which will allow the transferring of low-surface-energy components to the surface, leading to self-healing. For materials with a T_g below room temperature, this self-replenishing process will already happen automatically without additional heating, and the regeneration rate will only increase with climbing temperatures. In the systems discussed above, the polymer brush or segments are either covalently bound onto the substrates or form a crosslinked network, enabling the high stability of the materials. A potential drawback of all these examples fabricated through covalent grafting is, however, their slow self-replenishing process. In addition, the slow movement will also reduce the antifouling properties. Improvements can therefore be achieved in two ways: by either lowering the T_g of the polymer brush (as was, e.g., observed in the comparison between acrylate, methacrylate and random mixture polymer brushes by Wang and Zuilhof),[13b] or by fully replacing the bound polymer segments or brushes by dispersing low-surface energy small molecules in the main fixed matrix as the antifouling components. The latter is the approach taken in SLIPS.

Aizenberg's group extended the class of self-regeneration systems by dispersing low-surface energy compounds into porous materials to develop synthetic, liquid-repellent surfaces consisting of a film of lubricating liquid locked in place by a micro/nanoporous substrate.[15a] They fabricated two sets of SLIPS by incorporating low-surface tension perfluorinated liquids into arrays of nanoposts modified by a low-surface energy polyfluoroalkyl silane, and by incorporating such liquids in a random network of Teflon nanofibers distributed throughout the bulk substrate (**Figure 9**A). Each of these two SLIPS exhibits outstanding liquid repellency as verified by very low CA hysteresis and very low sliding angles against many

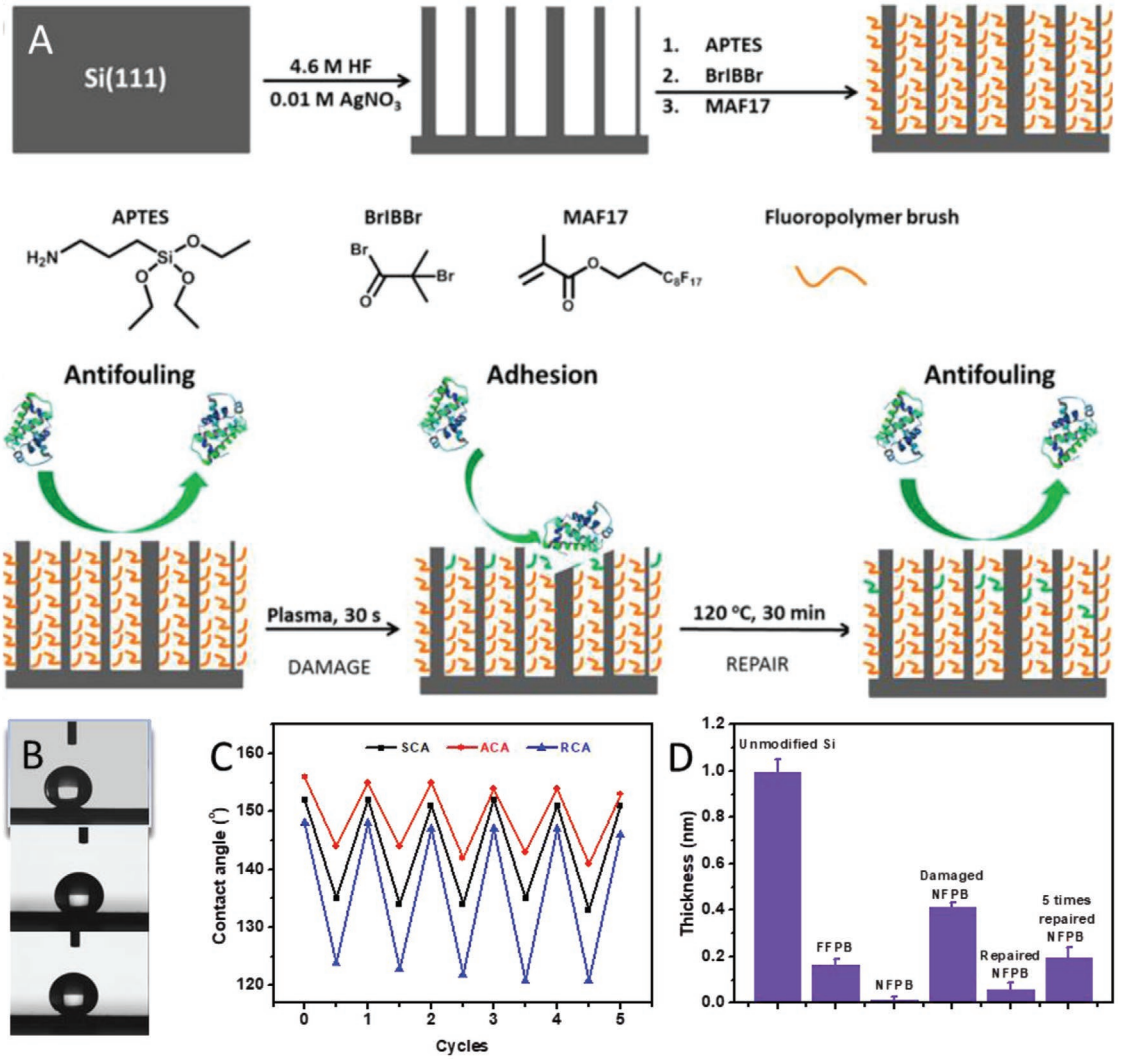

Figure 8. A) Schematic depiction of modified nanowire formation: nanowire fabrication, initiator immobilization, and covalent coating of the nanowires with a fluoropolymer brush. Subsequent: protein adhesion behavior on the original, damaged, and repaired polymer-coated Si nanowires. B) Static CA of original, damaged and repaired nanostructured PMAF17 brushes. C) The water static CA, advancing CA and receding CA changes of the nanostructured PMAF17 brush between plasma-induced damage and repair at 120 °C for 2 h. D) The increased thickness of BSA fouling on different surfaces as measured by XPS. FFPB and NFPB denote flat and nanostructured fluoropolymer brush. Reproduced with permission.[13c] Copyright 2016, American Chemical Society.

different kinds of liquids ranging from n-pentane to water (with surface tensions from 17 to 72 mN m^{-1} (Figure 9B). The lubricating films can also be utilized as self-healing coatings to quickly repair its liquid repellency upon abrasion or impact damage of these porous materials. The fluidic nature of the lubricating layer means that the lubricant can easily flow toward the damaged area due to surface energy-driven capillary action, and spontaneously refills small physical scratches in 150 ms at room temperature to repair the damage. Moreover, SLIPS can regenerate their liquid-repelling function multiple times upon repeated large-area damage (Figure 9C). Finally, SLIPS are also capable of effectively repelling complex fouling fluids, such as blood, which often rapidly wet and stain many surfaces, demonstrating outstanding antifouling properties.

Since the invention of the SLIPS, many different kinds of SLIPS were developed by other groups. The matrix materials can be nanostructured surfaces, crosslinked polymer networks, layer-by-layer assembled films, and so on. The lubricant can be low-molecular weight fluorinated compounds, silicones or ionic liquids. Designing a SLIPS is mainly based on the following three considerations: 1) the lubricant can wick into, wet and stably adhere within the matrix smoothly, 2) the solid must be preferentially wetted by the lubricating liquid rather than by the fouling media, and 3) the lubricating and fouling media should not mix. The SLIPS can be fabricated by the two following approaches: a) filling the lubricant into the as-prepared porous materials and b) polymerizing or curing the lubricant and precursor solution together to obtain the composite SLIPS. Based on the abovementioned three criteria and two methods, many different self-healing and antifouling SLIPS materials have been developed in recent years, such as silicon–oil infused silicone,[47] silicon–oil infused 3D vascular systems,[48] silicon

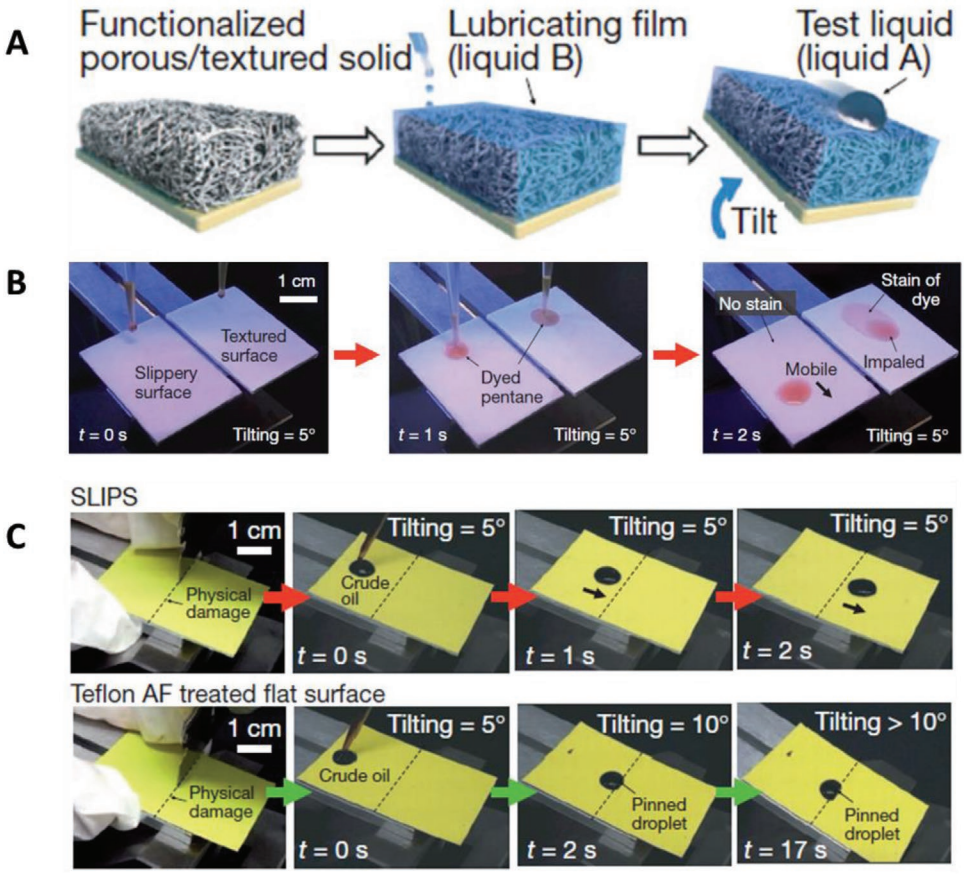

Figure 9. A) Schematics showing the fabrication of a SLIPS. B) Movement of pentane droplets over time on SLIPS and superhydrophobic surfaces. C) Rapid repair of damaged SLIPS surfaces (compared to a typical hydrophobic flat surface) as shown from drops rolling past a scratch. Reproduced with permission.[15a] Copyright 2011, Nature Publishing Group.

oil infused chemical etched stainless steel,[49] oil-impregnated nanoporous oxide layer,[50] perfluorinated fluid-filled porous Teflon,[51] Krytox 100-infused porous Zn–Ni–Co,[52] perfluorinated lubricant immobilized 3D fibrous network,[53] perfluorooctanoate-infused polyelectrolyte multilayer films[54] and fluorinated ionic liquid gels.[55] In all these systems, the lubricant will automatically replenish the surface and effect SHAF properties.

In the SLIPS systems discussed above, the lubricants have relatively weak interactions with the matrix materials. This indeed leads to fast antifouling and self-healing behavior, but also to the leakage of lubricant upon use. To minimize lubricant leakage and on-demand release of the lubricant upon external stimuli, the lubricant can be prestored in the matrix and released upon external stimuli such as temperature and UV light.[56] Alternatively, binding lubricant inside the polymer networks to fabricate organogels or using solid lubricants can provide a solution. Inspired by the regenerable solid epicuticular wax on the surface of pitcher plants, a self-replenishing organogel (OG) material was prepared by Wang, Jiang and coworkers through immersing a porous crosslinked PDMS-based material into crude oil (**Figure 10**A). When molten paraffin wax was deposited on the OG surface at room temperature, it was repelled, spread and became un-transparent. After 21 s, the OG surface was slightly tilted and the solidified paraffin wax moved smoothly downward (see the various pictures taken from 0 to 52 s after deposition of the paraffin; Figure 10B), indicating that the OG displays an excellent repellence against the paraffin wax. However, the solidified paraffin wax quickly stuck on a solid PDMS surface at the place of deposition (Figure 10B) and indicating strong interactions and concomitant severe fouling. The fact that heterogeneous nucleation can be avoided by the OG surface is believed to contribute to this ultra-low adhesion. The OG material displayed self-replenishing ability through catching small molecular compound during crude-oil flowing, which is similar to fish and pitcher plants that can grab water molecules nearby.[57] The same approaches were also used by Zhang and co-workers to fabricate an OG that combines SHAF characteristics with efficient inhibition of bacterial adhesion and a high optical underwater transmittance. Studies on the effect of the chain length of *n*-alkanes on bacterial inhibition behavior showed that the OG with *n*-alkanes of shorter chain (comparing between *n*-dodecane, *n*-tetradecane, and *n*-hexadecane) exhibited better performance in bacterial inhibition.[58]

The key point to develop high-performance antiadhesion organogels is to guarantee the liquid surface layer that blocks direct contact between foulant and surfaces can be preserved for a long lime. Ideally, one thus creates a reservoir containing a significant amount of liquid in the crosslinked network, so that this surface layer can be maintained.[59] However, although

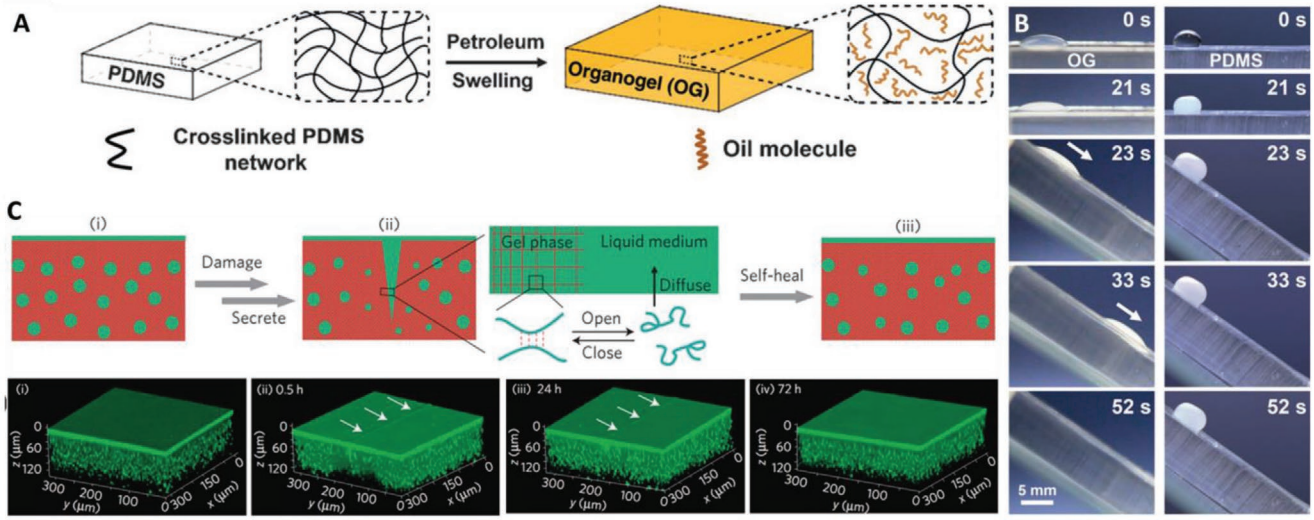

Figure 10. A) Crosslinked PDMS immersed in petroleum, resulting in the diffusion of oil molecules into the crosslinked network and swelling of the PDMS. B) Solidified paraffin wax easily slides from an OG surface, but is pinned on solid PDMS. Reproduced with permission.[57] Copyright 2015, Wiley-VCH. C) Schematic model of secretion-mediated response to scratching the polymer, as based on confocal fluorescence images of a damaged PDMS-based organogel over time. Reproduced with permission.[60] Copyright 2015, Nature Publishing Group.

organogels can block the lubricant leakage to some extent, the stability of the liquid lubricating layer still deserves careful considerations. In response, Howell et al. developed a kind of vascular network-encased organogel materials to minimize the evaporation that leads to loss of liquid. Such a "vascular" system can act as an internal reservoir, and as such still allows for the continuous regeneration of the surface layer, but with a strongly reduced loss of lubricant.[48]

To obtain more control over the release of the liquid, Cui, Aizenberg and co-workers designed a supramolecular organogel that was crosslinked by dynamic intermolecular hydrogen bonds with a self-regulated liquid surface layer with silicon oil lubricant droplets stored within the polymer matrix. The disjoining pressure generated from the apolar liquid in the (polar) H-bonded supramolecular polymer network will keep the liquid surface layer thickness between ten and hundreds of nanometers. This oil film thickness can thus be regenerated through disjoining pressure-induced lubricant secretion upon disturbing or removing the surface oil layer.[60] Upon mechanical scratching, this organogel will autonomously self-heal due to the reversible cleavage and reformation of H-bonds within the supramolecular polymer network (see Figure 10C). To mimic the lubricating capability of earthworms, which secrete lubricants in fast response to observed friction, they extended their study to develop a textured structure on the surface of liquid-releasable polymer coatings by a "breath figure" process.[61] The resulting coatings can release oil at specific sites upon external stimuli such as solid-based friction, which will form an oil layer that can be stabilized by the textured surface, further reducing friction and enhancing wear resistance. Moreover, the coatings also exhibit excellent antifouling behavior in a sticky soil environment.

Another way to improve the stability of the SLIPS materials is to use a solid lubricant. For example, organogels made from crosslinked PDMS and molten alkanes can prevent the deposition of foreign materials, so as to obtain antigraffiti, antifouling, and anti-icing properties, due to the easy removal of the sacrificial solid alkane layer. This coating also demonstrates a long lifetime, as the sacrificial layer can be easily regenerated, such that, e.g., the anti-icing property was maintained even after 20 icing/deicing cycles or sandpaper abrasions.[62] Heng and co-workers developed a solid slippery surface composed of paraffin wax and a porous polystyrene film. Droplets of several liquids with different surface tensions can slide over the surface without staining it. Utilization of a solid alkane-based lubricant enabled this solid slippery surface much better stability than SLIPSs, as evidenced from immersions in different pH solutions. Significantly, these solid-infused surfaces can rapidly self-heal from physical damage via a heating–cooling process, because the underlying porous polystyrene matrix firmly locks the paraffin even when the latter is liquid.[63] Similar results have been obtained by Clancy and co-workers using solid perfluoroalkanes as the lubricant to fabricate polydimethylsiloxane gels capable of regenerating deicing surfaces.[64] However, while functioning well, the easy loss of perfluoroalkanes into the environment would strongly hamper this use, especially given the success of simple paraffin wax.

2.1.2. Surface Regeneration of High-Surface-Energy Materials in Aqueous Environments

Self-regeneration of these low-surface-energy materials is normally achieved in air, which steers to minimize the surface energy to achieve the most stable materials. Water-induced surface regeneration should therefore rely on different driving forces, and is highly interesting since antifouling properties are in high demand in aqueous environments. For example, a pH-responsive poly(2-vinylpyridine) film with a 3D grafting of poly(ethylene oxide) on it demonstrated a four-fold increase in the lifetime of its antifouling characteristics compared with the same material with only the surface-grafted polymer.[65] The

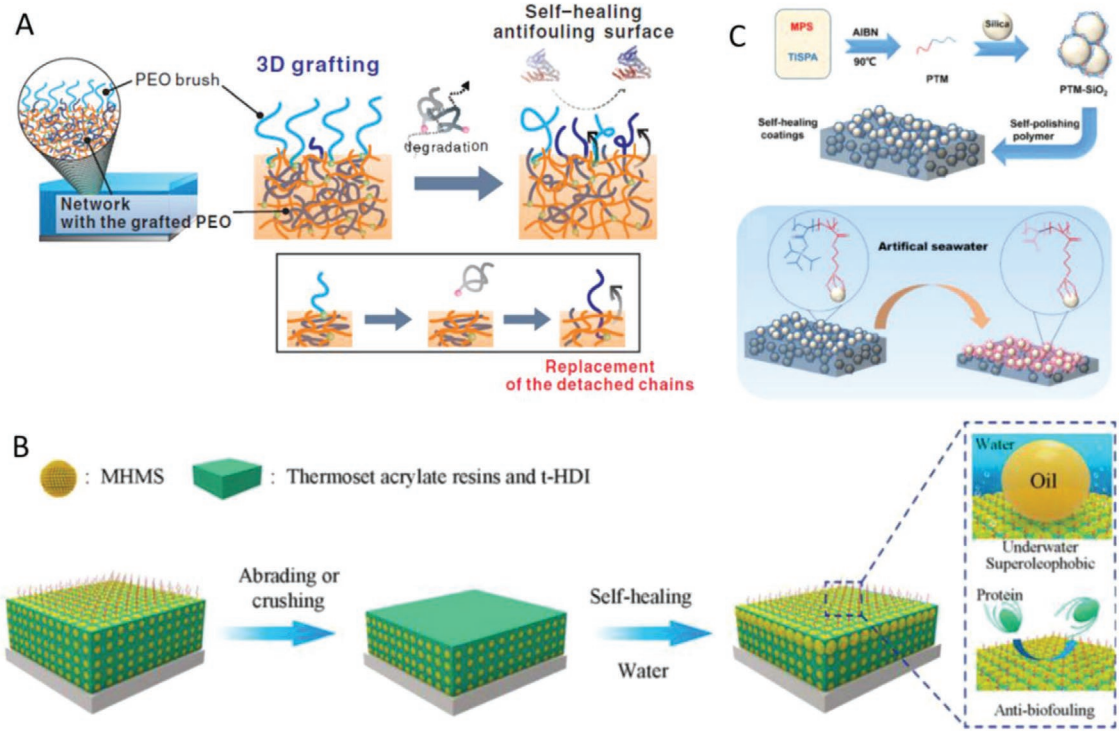

Figure 11. A) 3D polymer grafting on the surface and inside of a P2VP film. Reproduced with permission.[65] Copyright 2013, Wiley-VCH. B) Working principle of the self-repairing underwater superoleophobic/antifouling coating of Wu et al. Reproduced with permission.[66] Copyright 2016, American Chemical Society. C) Schematic diagram of the fabrication strategy of seawater-induced underwater superoleophobic coatings. Reproduced with permission.[67] Copyright 2019, American Chemical Society.

coating was 3D grafted by polymer chains, both at the surface and inside the polymeric host material, allowing it to retain its antifouling property even after removing a big part of the attached polymers (**Figure 11**A). The self-healing mechanism of the proposed structure relies on the replacement of the detached or damaged polymeric chains by relocating segments of the chains stored inside the film close to the interface: upon loss of the polar chains, there is an emerging gradient in the chemical potential that drives this relocation, with as desired effect the recovery of the antifouling behavior in the exposed area. This is effectively the same mechanism as noted before for apolar layers in air or organic polymer solutions.[13a,c,31] In a similar way, Wu's group prepared PEG-*b*-PHEMA-*b*-PMPC triblock copolymers that were grafted onto both the surface and the inside of polyurethane base coatings, to obtain hydrophilic polymer 3D-grafted films. These functionalized polymers displayed a strong inhibition of protein and human platelet cell attachment. After the surfaces were chemically or mechanically damaged, the hydrophilic polymer chains stored inside the coatings would again relocate, effecting repair of the surfaces and allowing it to maintain a long-term antifouling ability in the underwater environment.[68] Esteves et al. reported a somewhat analogous multiblock hydrophilic polycarbonate-poly(ethylene glycol)-polyurethane coating, which displayed stability, a high protein repellence and regeneratability of the protein antiadhesion property owing to the dangling hydrophilic chains incorporated in the bulk materials beforehand. It was confirmed that the combination of a low T_g and sufficient mobility of the PEG dangling chains is essential to affect the autonomous recovery of the surface hydrophilicity when the coatings were immersed in water.[69]

The goals of such coatings can even be further extended to include both anti-biofouling as well as oil-repelling characteristics. To such an aim, Wu et al. prepared a self-healing underwater–oil repellent and biofouling-resistant coating consisting of SiO_2 microspheres that were covered with an ABC triblock polymer [poly-(methacryloxy propyl trimethoxyl silane)-*block*-(poly-(hydroxyethyl methyl acrylate)-*co*-poly(2-methacryloyloxyethyl phosphorylcholine)]. This mixture self-assembled on a glass substrate, and was subsequently fixated by spin-coating a thin layer of a thermosetting acryl-based resin with 1,6-hexamethylene diisocyanate trimer as a crosslinker. The superfluous upper part of the resin was removed by rinsing with ethyl acetate, and the remaining system was cured at 80 °C to obtain a self-repairing underwater superoleophobic and anti-biofouling coating (Figure 11B).[66] When subjected to physical damage (abrasion under 10 kPa), this leads to significant interaction with oily components, but the materials can fully recover its underwater–oil nonadhesion upon immersion in water for 12 h. The coating exhibits a relatively low BSA adsorption of about 3 μg cm^{-2}, which remains low after abrasion and repair (<10 μg cm^{-2}), suggesting that these coating also has long-term anti-biofouling properties in a marine environment. An analogous nanoparticle-including approach was reported by Wang and co-workers, which used nanocomposites consisting of a bulk biocompatible polymer, polycaprolactone (PCL),

mixed with a small fraction (1–3 wt%) of polymeric nanoparticles consisting of a hyaluronic acid (HA)-PCL graft copolymer (HA-g-PCL). Upon immersion into an aqueous buffer, the hydrophilic chains of HA will move toward the interface between the HA-g-PCL nanoparticles and water, which presents a hydrophilic "slimy/artificial mucus" layer at the surface of this material, which induces the regenerated PCL film to display excellent protein repellence and cell antiadhesion property. Upon mechanical abrasion, this regeneration process will rehappen again, retaining the surface's protein/cell resistance.[70] Zhou et al. developed a seawater-induced strategy to create in situ an underwater superoleophobic surface, starting with water-responsive polymer-grafted SiO_2 nanoparticles that were embedded in a self-polishing polymer (Figure 11C). When brought into contact with seawater, the surface was slowly and partially hydrolyzed, and as such renewed the outside of this sacrificial self-polishing polymer and its subsequent dissolution. Particularly, hydrolysis of grafted apolar poly(triisopropylsilyl acrylate-*co*-3-methacryloxy-propyltrimethoxysilane) chains provides hydrophilic segments, which in addition effect a minimal adhesion toward oil, and also provide the surface with antiprotein adsorption features.[67]

From the discussion above we can see that the components or moieties responsible for self-replenishing processes can be stored into a matrix by 3D grafting, infusing and encapsulating. The components can either be covalently bound onto or into the network, or are loosely dispersed within the matrix. Covalent grafting endows the components high stability, but again at the expense of a somewhat slower regeneration; when the responsible components are dispersed inside the matrix by infusion, the regeneration can finish in seconds, but with the drawback of an inevitable leakage of the infused materials upon use of the material. In future studies, a weak bonding between the responsible component and matrix network induced by supramolecular interactions such as multiple H-bonding and π–π stacking could be an alternative choice to fine-tune the speed of action and stability of such self-replenishing antifouling materials.

2.2. Repair of Structural/Shape Damage by Reversible Covalent and Noncovalent Interactions (Category II)

In the first part, we discussed self-replenishing surfaces, which after loss of material by abrasion-induced wear or chemical degradation regenerate the original surface chemical composition. Self-healing thus referred to the surface composition and function recovery, but not to recovery of, e.g., shape, as the loss of material prevents a full recovery of the structure. Such recovery of both function and shape is crucial for the repair of scratches or cracks with micrometer-scale sizes. This damage is visually hard to see, but will result in the loss of function in this microscale-damaged area. Foulants are easily trapped in such scratches/cracks, leading to further fouling. In recent years, many studies related to this kind of self-healing antifouling materials were developed, which is discussed in the current section.

Sun's group utilizes PEI and PAA to fabricate a self-healing polyelectrolyte multilayer (PEM) coating based on electrostatic interactions. This coating can repair itself upon mechanical scratching with the aid of water.[71] The self-healing mechanism originates from the easy flow of the water-swelled coatings and the interdiffusion of polyelectrolytes at the fractured surfaces. This study reported a typical method to fabricate self-healing PEM coatings; by introducing other polymer materials with functional groups, many kinds of functional self-healing PEM coatings can be fabricated. In a subsequent study, they modified a branched PEI by grafting PEG and fabricated a PEI-PEG/HA-PEM film, which also possessed excellent self-healing, and—because of the PEG—also anti-biofouling properties (**Figure 12**A). This anti-biofouling property was also repaired during the self-healing processes (Figure 12B,C).[72]

By using the same method, they prepared SHAF polymeric films via a layer-by-layer assembly (LbL; 100 double layers) of partially hydrolyzed poly(2-ethyl-2-oxazoline) (PEtOx-EI-7%) and PAA with H-bonding interactions as the main driving force.[75] The thermally crosslinked PAA/PEtOx-EI-7% films displayed strong resistance to bacterial adhesion by both Gram-negative *Escherichia coli* and Gram-positive *Bacillus subtilis*. This was stated to result from the high fraction of the antifouling polymer PEtOx-EI-7% throughout the entire coating, although PAA itself might also have contributed. In addition, rapid self-healing was obtained: upon application of a mechanical cut at microscale, the crosslinked films were repaired fast by immersing the coatings into water, which was affected by the reversibility of H-bonding and high polymer segment mobility in water. Similarly, antibacterial films with high transparency that are capable of healing scratches and restoring the optical transmittance were fabricated by an exponential layer-by-layer assembly of branched polyethylenimine (bPEI)/PAA films and postdiffusion of cetyltrimethylammonium bromide micelles encapsulated with antibacterial agent triclosan.[26a]

Chen et al. fabricated another kind of SHAF coatings by adding capsaicin@chitosan (CAP@CS) nanocapsules into polydopamine/sodium alginate (PDA/Alg)m PEM films. These coatings can be triggered by pH to release the antifouling agent CAP. The electrostatic interaction between Alg and PDA effects (PDA/Alg-CAP@CS-n)m films to exhibit self-healing behavior, since the polyions interpenetrate, and allow polymer chains to transfer to the surface in artificial seawater solutions after mechanical scratching (Figure 12D,E). Colonies of bacteria on original and healed PEM films remain at a low quantity (84–91% reduction against *Staphylococcus aureus* and *Pseudomonas aeruginosa*, respectively) compared with blank samples after cultivating for 18 h (Figure 12F). This antibacterial action of multilayers after a damage-healing cycle only decreases by around 5% (Figure 12G).[73] LbL assembly of sulfonated hyperbranched polyglycerol and quaternized polyethylenimine onto poly(ether sulfone) membranes that were pretreated with polydopamine to facilitate the LbL process, also provided excellent self-healing and antifouling properties.[76] The LbL method could also be used to fabricate a healable bactericidal coating via immobilization of hydrophobic antimicrobial peptides into a multilayer film, which was constructed through an enhanced exponential LbL assembly of polyethylenimine and poly(acrylic acid).[77]

LbL is indeed a nice method to fabricate water-repairable PEM coatings with great potential antifouling properties, but

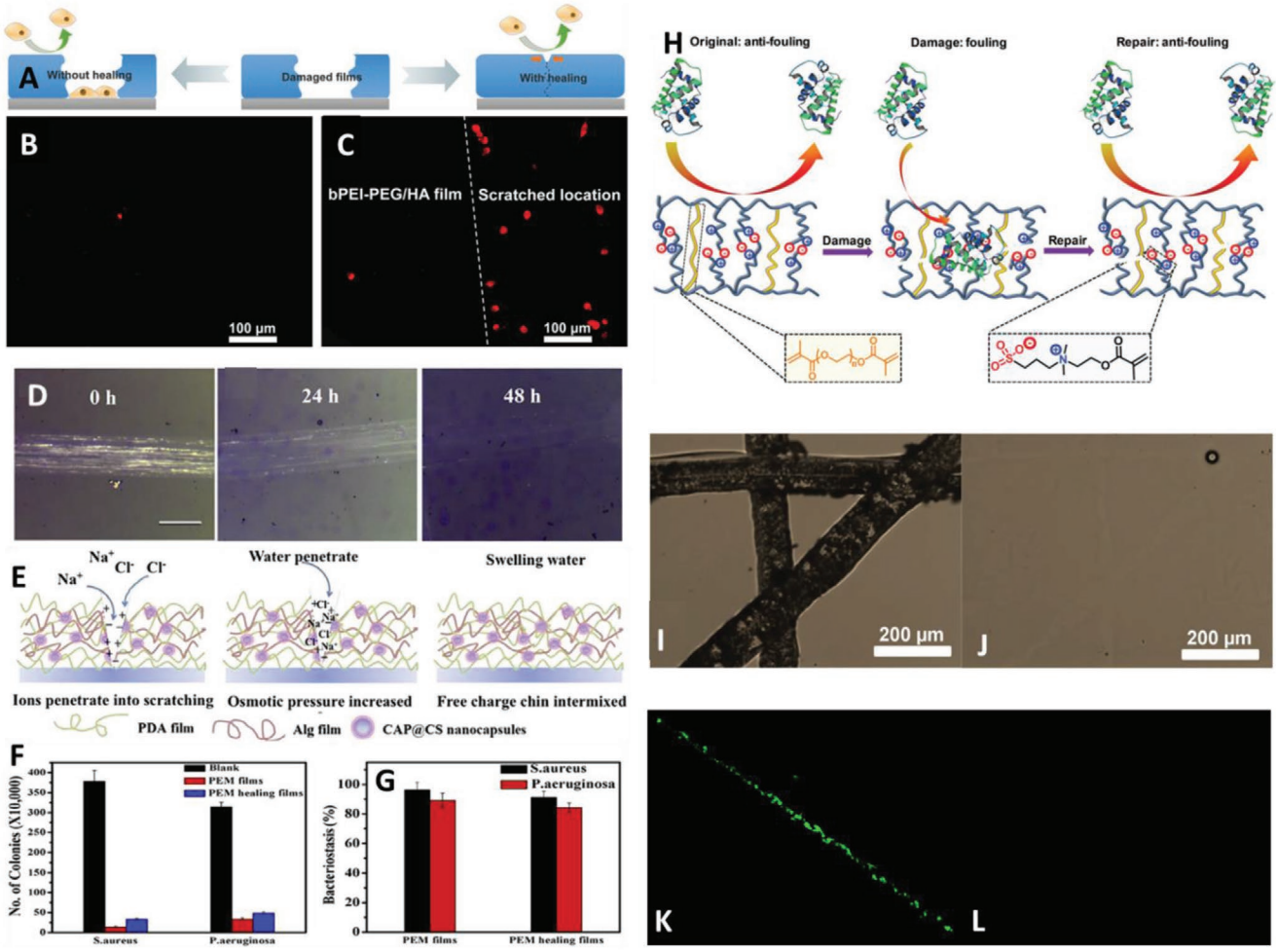

Figure 12. A) Damage–repair cycles of healable antifouling films assembled from PEI-PEG and HA. Cell adhesion on the healed B) and scratched C) PEI-PEG/HA films. Reproduced with permission.[72] Copyright 2015, Wiley-VCH. D) Microscopy images of the repair of a $(PDA/Alg\text{-}CAP@CS\text{-}8)_{20}$ multilayer film upon immersion in water for 0, 24, and 48 h. E) Schematic diagram of self-healing procedure of $(PDA/Alg\text{-}CAP@CS\text{-}8)_{20}$ multilayer film in artificial seawater. F) The number of *S. aureus* and *P. aeruginosa* bacteria in Luria–Bertani medium for 18 h with different modified substrates. G) The bacteriostasis of PEM films against *S. aureus* and *P. aeruginosa*. Reproduced with permission.[73] Copyright 2019, Elsevier. H) Monomer structures used to prepare zwitterionic polymer networks (ZPNs) and the protein adhesion behavior on the original, damaged, and repaired ZPNs. Optical images of mechanically damaged ZPN coatings I) and after immersion (1 min) in water for 1 min and subsequent drying J). Fluorescence images of the damaged K) and repaired L) ZPN coatings after immersion into an Alexa 488-BSA solution for 10 min. Reproduced with permission.[74] Copyright 2017, Royal Society of Chemistry.

a drawback of this method is that it is rather time-consuming, while thus fabricated coatings are always very thin, normally in nanometer scale. Overcoming this limitation, Wang and co-workers prepared a zwitterionic polymer coating by drop-casting or spin-coating a polymer solution through copolymerization of 2-[(methacryloyloxy)ethyl]dimethyl-(3-sulfopropyl)ammonium hydroxide and poly(ethylene glycol)dimethacrylate (Figure 12H). These coatings can self-heal in water within 1 min upon mechanical scratching (Figure 12I,J). Even if the film is thin, down to a nanoscale thickness of 80 nm, this coating still displays excellent self-healing. Due to the super- hydrophilic character of the zwitterionic groups, this coating also displayed good protein-repellent properties, and this protein repellence was also repaired during the self-healing process (Figure 12K,L).[74] The reaction of a linear polyacrylate resin containing pendent sulfobetaine and acetoacetyloxy groups with an amine-functionalized hyperbranched polysiloxane (HPSi) can be used to form a multifunctional crosslinked polyacrylate coating. This coating shows a high mechanical strength, and reversible self-healing and antibacterial abilities through dynamic vinylogous urethane groups.[78] An antibacterial and self-healing Soy protein isolate-based material with high mechanical strength was fabricated by integrating polyethyleneimine and metal ions in it.[79] Autonomous self-healing ice-resistant coatings based on dynamic coordination bonds were also reported by Zhang and co-workers.[80] Liu et al. developed a self-repairing coating which is composed of poly(dimethylsiloxane) based polyurea (PDMS-PUa) and a small percentage of organic antifoulant (4,5-dichloro-2-*n*-octyl-4-isothiazolin-3-one) (DCOIT). The coating can fully recover its mechanical properties after damage either in air or artificial seawater at room temperature due to the reversible hydrogen bonding. In addition, six-month marine field tests (at the inner Xiamen

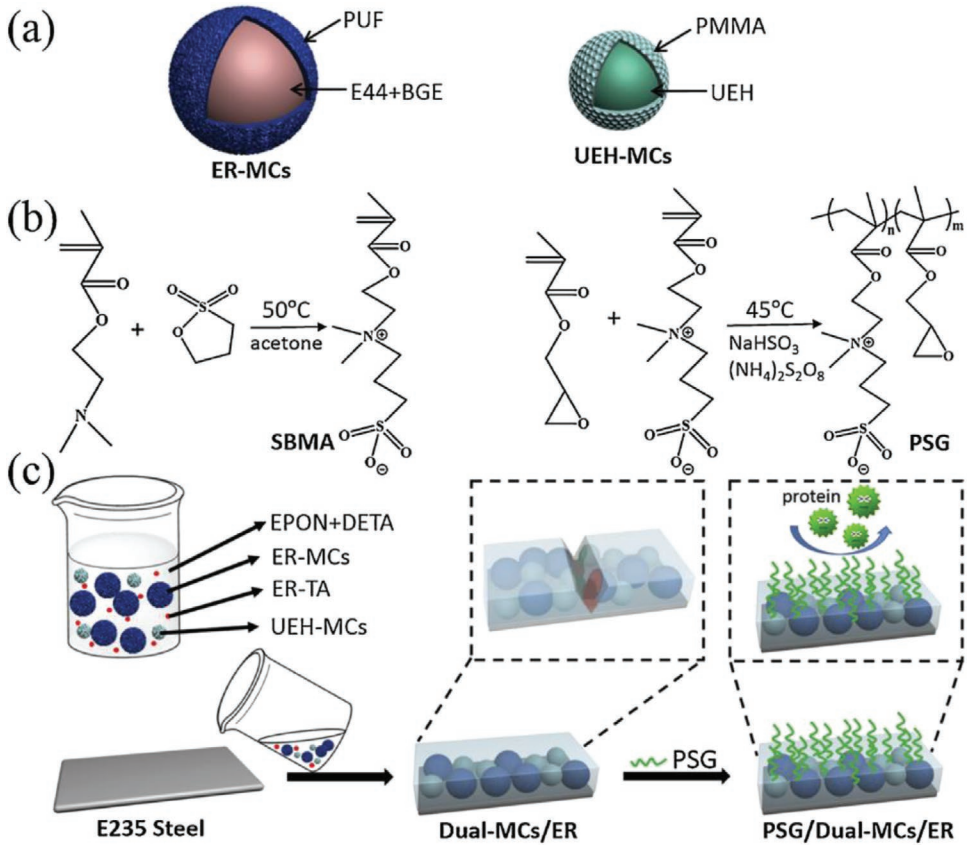

Figure 13. a) Structures of epoxy microcapsules (ER-MCs) and underwater epoxy-hardened microcapsules (UEH-MCs). b) Synthetic route toward sulfobetaine methacrylate (SBMA) monomer and zwitterionic poly(sulfobetaine methacrylate-*co*-glycidyl methacrylate) (PSG). c) Formation of the PSG/dual-MCs/ER coating. Reproduced with permission.[82] Copyright 2019, Elsevier.

bay) demonstrate that the system possesses a good antifouling/fouling release performance even upon prolonged natural underwater exposure. For marine testing, such long-term experiments are very much needed to properly evaluate the potential of the systems at hand. The combination of the fouling-release performance of PDMS-PUa, the slow release of the antifouling agent, and the autonomous self-healing property is responsible for this long-term antifouling performance in a relatively harsh marine environment.[81]

Micro/nanoscale scratches can also be repaired by internally storing a healing reagent that can flow into the damaged area, polymerize and solidify to repair the damage. Dong and coworkers developed a dual-functional coating with underwater self-healing and protein-repellence properties by integrating two kinds of microcapsules and a zwitterionic copolymer together (**Figure 13**). Epoxy resin microcapsules and underwater epoxy hardener microcapsules were mixed with an amine-cured epoxy coating system to cast a coating on steel. Subsequently, a poly(sulfobetaine methacrylate-*co*-glycidyl methacrylate) (PSG) solution was casted on the surface of the un-cured epoxy coating. The coatings fabricated by this method displayed excellent SHAF characteristics, effected by the dual microcapsules and the anti-protein-fouling performance provided by PSG.[82]

Overall, it is clear that micro/nanocracks or scratches will cause surface fouling during the service lifetime of many materials. Developing automatically self-healing systems or materials that can be repaired by getting energy from the environment they are used in is the most interesting. In this regard, especially water-induced self-repair of anti-biofouling materials deserves to be studied more extensively, as anti-biofouling materials are always used in aqueous environment. Highly relevant here is a high rate of repair, as fouling onto damaged areas will both hamper the repair and induce further fouling. Activated healing processes, such as those requiring heating, are less interesting in this case, as the small scale of such damages are difficult to be observed, and thus fouling will often be induced, with both loss of function and structural integrity.

2.3. Combination of Surface Replenishing and Scratch Repair (Category III)

The long-term use of materials can typically not be predicted, and as such also the type and degree of damage. To thus allow a wide variety of usage conditions, new kinds of anti-biofouling polymer materials integrating a self-healing structure, high mechanical strength and optimal surface properties all at once are of great interest. Such materials, which thus combine the properties of the previously discussed categories I and II, to (start to) populate this most stringent category III class of materials, need to possess the balance between being flexible enough to allow molecular mobility on one hand, and sufficient

structural strength to withstand substantial abrasion and surface restructuring on the other hand.

Yang and co-workers prepared reactive or nonreactive liquid cores in resorcinol-modified poly(urea-formaldehyde) (PUF) microcapsules (MCs) with excellent resistance to non- or less-polar solvents and thermal stability through a facile one-pot microencapsulation method.[83] Particularly, MCs containing hexamethylene diisocyanate (HDI) as a moisture-sensitive healant exhibited very good superhydrophobicity. SHAF coatings could be affected by dispersing the HDI-filled MCs in an epoxy matrix. The large fraction of amino and hydroxyl groups immobilized on the surfaces of PUF particles during the formation of PUF MCs endow the freshly prepared HDI MCs excellent hydrophilicity. Furthermore, carbamic acids generated by the reaction between HDI and water/moisture are not stable, but can further composed into amine groups that can further react with HDI to form polyurea. As a result, the surface gradually transformed from hydrophilic to superhydrophobic (**Figure 14A**1). When dispersed in a polymer matrix, self-healing was realized by the release of HDI which with the aid of water can form polyureas to fill the cracks (Figure 14A2). After experiencing serious damage, e.g., by plasma etching, the coating can recover to a superhydrophobic state, again simply under ambient conditions at room temperature (Figure 14A3).

Wang and co-workers reported the first kind of dual self-healing anti-biofouling coating that can self-repair damage at both macro- and nano/microscales and recover both surface wetting and anti-biofouling properties (Figure 14B).[84] When a damaged surface with a thin cut is immersed in a fluorescent protein solution, the protein adheres onto the damaged area, as manifested by a locally intense green fluorescence (Figure 14C1,C2). After being repaired in salt water at room temperature, no protein adsorption at all is observed in the initially damaged area (Figure 14C3,C4). In the case of macro damage, for example by removing the top layer with a razor on purpose, again strong protein adsorption happened (Figure 14C5,C6). Repair of these macrodamaged coatings just required immersing them into salt water, and effected full recovery of the anti-biofouling properties (no protein adsorption visible; Figure 14C7,C8). We hypothesized that upon nano/micromechanical scratches, the broken ionic bond between the protonated ammonium group and sulfonic group can be reformed again via the involvement of aqueous salt solutions, which thereby repairs the damage. The anti-biofouling properties during this damage-repair process should then also be repaired. This mechanism falls short for larger, macroscale damage, as the long distance prevents the broken chains from reformation. However, the 3D structure of these coatings allows for a slow reorientation toward the surface of buried zwitterionic groups when brought in contact with salt water, with the regeneration of the surface-wetting properties and the concomitant recovery of its anti-biofouling character.

Li et al. prepared transparent antismudge coatings with a heating-assisted healing ability using 1H,1H,2H,2H-perfluorodecanethiol (PFDT) grafted 1,2-polybutadiene (PB) (Figure 14D).[85] Many kinds of liquids with different surface tensions can slide off from the coating completely due to the polyfluorinated chains present at the surface. For example, a decane droplet was firmly pinned on the PB-g-PFDT3 coating after the coating was etched by O_2 plasma for 5 s (Figure 14E1,E2), as the O_2 plasma rapidly destroyed the PFDT groups on the coating surface. Interestingly, such a decane droplet could easily slide down the plasma-etched PB-g-PFDT3 coating after storing the coating under ambient conditions for 48 h (Figure 14F1,F2), showing that these coatings possess autonomous self-healing behavior against the oxidation-induced decrease of its liquid repellency. This self-healing behavior was driven by the migration of PFDT groups stored in the bulk coating to the damage area to minimize the surface energy. Owing to the oleophilicity of the substrate, a decane droplet was firmly pinned at a microscale cut while sliding off the damaged PB-g-PFDT3 coating (Figure 14G1). Heating the damaged PB-g-PFDT coating at 80 °C enables the cut gradually disappear within 5 min, and the decane droplet could easily slide off the healed PB-g-PFDT3 coating again without any pinning (Figure 14G2), indicating the successful healing of the cut.

Such dual-scale SHAF behavior has also been achieved by slippery organogels (OG). To this aim, a linear poly(dimethylsiloxane)-based polyurea (PDMS-PUa) was prepared through the coupling reaction between α,ω-aminopropyl-terminated poly(dimethylsiloxane) (APT-PDMS) and isophorone diisocyanate (IPDI). A slippery OG coating was made by mixing PDMS-PUa and silicone oil, which can be stably trapped in the gel through H-bonding. The reversible breaking and reforming of hydrogen bonding in urea groups between PDMS-PUa endows the OG with these self-healing characteristics. Migration of silicone oil through the PDMS-PUa matrix to the damaged area can regenerate the lubricant oil layer. The as-prepared OG presented an impressive liquid-repellency performance with a low tilted angle of <10°. The healed liquid repellence of the OG is due to the self-healing of the PUa substrate and the self-regeneration of the lubricant oil layer. Furthermore, under both static and dynamic environments, the OG layer provided an excellent antifouling performance against bacteria in a culture solution compared with the background and with PDMS-PUa (without oil).[86] This OG material is very similar to that mentioned in the Category II, however, the previous systems do not display a dual self-healing antifouling function. Ramakrishna et al. demonstrated the possibility to obtain a melt-processable, dual SHAF coating by drop-coating long alkyl (octadecyl) chains grafted silica nanoparticle. The well-defined nanomaterial shows superhydrophobicity in the bulk and is able to heal macrocracks upon gentle heating. It can retain its wettability characteristics even after abrasion with a sanding paper. The surface quickly self-regenerates the superhydrophobicity (due to the reversible self-assembly of nanostructures) at ambient temperature even after, e.g., being treated with boiling water and multiple finger rubbing tests.[87] Silicon oil-infused poly (glycidyl methacrylate)-*co*-polydimethylsiloxane propyl ether methacrylate, which was crosslinked by magnetic Fe_3O_4 nanoparticles containing reversible coordination bonds, also displayed excellent dual SHAF properties,[88] including recovery of most of its mechanical strength upon repair after damage. The authors do not mention the self-replenishing property of this material, but due to the storage of silicone oil in the matrix, this coating will likely also repair the surface wetting and anti-fouling properties upon surface wear or degradation due to the regeneration of the silicone oil layer.

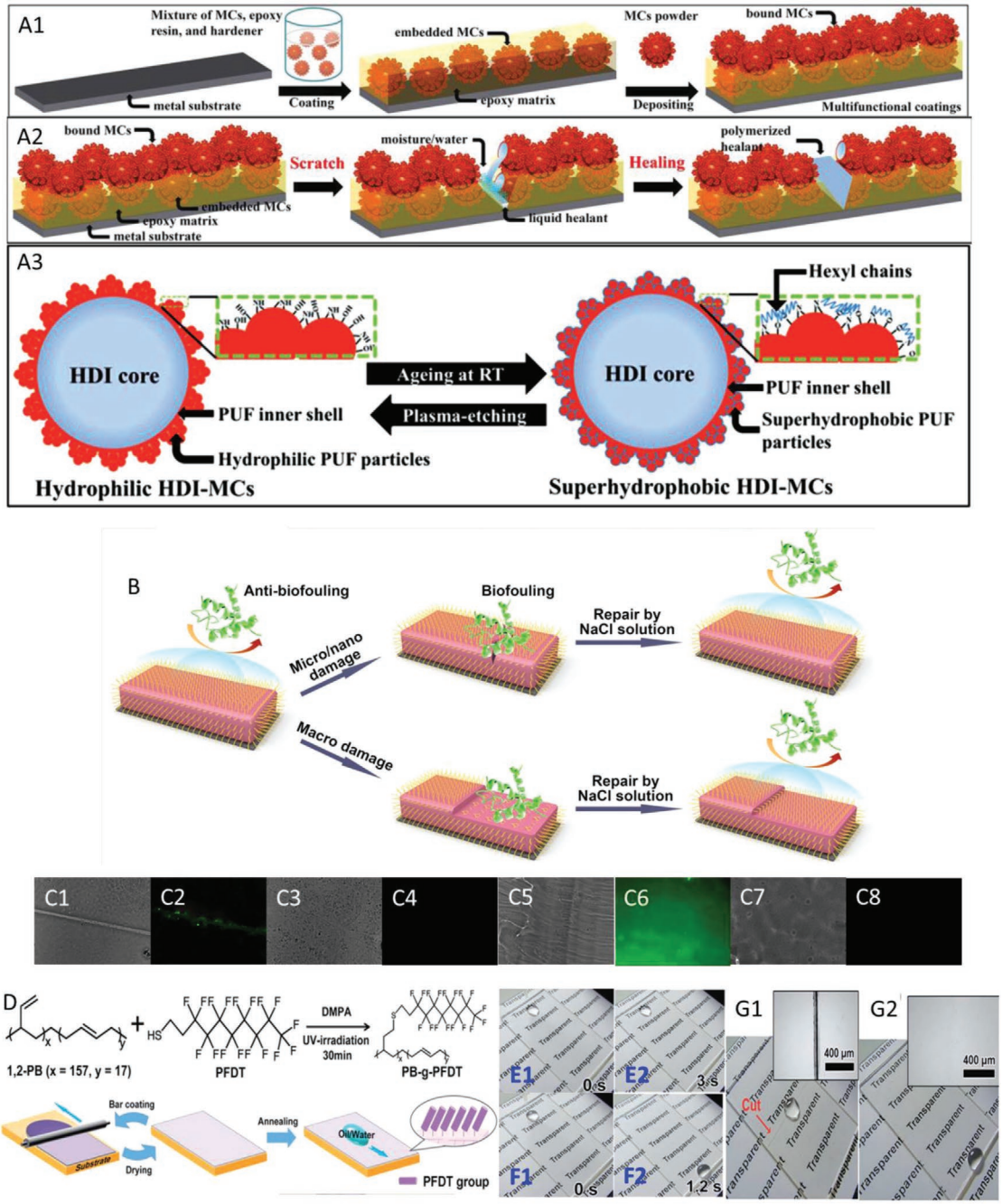

Figure 14. A1) Procedure to prepare HDI-filled microcapsule (MC)-based multifunctional coatings. A2) Schematic of the self-healing process of multifunctional coatings upon mechanical scratching. A3) Mechanism of the reversible hydrophilic–superhydrophobic transition of HDI-MC coatings. Reproduced with permission.[83] Copyright 2014, Wiley-VCH. B) Depiction of the protein-adhesion behavior on the original, damaged, and repaired zwitterionic polymer networks (ZPNs). C) Optical (C1, C3, C5, and C7) and fluorescence (C2, C4, C6, and C8) images of the microscale (C1–C4) and macro scale (C5–C8) damaged (C1, C2, C5, and C6) and repaired (C3, C4, C7, and C8) ZPN coatings after immersion into Alexa 488-BSA solution. Reproduced with permission.[84] Copyright 2018, Royal Society of Chemistry. D) Synthetic route toward PB-g-PFDT polymer and coatings. Sliding of decane droplets over the plasma-etched PB-g-PFDT coating before E1,E2) and after F1,F2) healing under ambient conditions. Photographs of decane droplets sliding on the cut PB-g-PFDT3 coating before G1) and after G2) healing. Insets: Microscopy images of the cut before G1) and after G2) healing. Reproduced with permission.[85] Copyright 2019, Royal Society of Chemistry.

After carefully reviewing the as-developed dual self-healing systems, we thus found that there are two main kinds of these materials: dynamic organic gels with low-surface energy liquids infused into it, and coatings made of the zwitterionic materials or PEG that were encapsulated and/or embedded into a materials matrix. The drawback of the first category is the weak adhesion between the materials and the surfaces. This drawback does not hold for the second category, but at the price of a somewhat more

complicated synthesis and detailed materials design. Future studies in this field might be focused on the design of new systems that combine a simple synthetic approach with strong interactions with the surface. Underneath such design should be an improved understanding of how the degree of fouling is dependent on the nature, size, and shape of structural damages. At the moment such an understanding is still in its infancy, suggesting there is lot to be improved for such SHAF materials.

3. Applications

SHAF materials have attracted great attention for protective coatings, oil/water separation and biomedical applications. Meanwhile, to extend their potential toward biomedical applications such as injectable hydrogels and biosensor surfaces, apart from a healable structure and antifouling characteristics, typical factors such as biocompatibility, the ability to be degraded in a natural fashion, stimuli-responsiveness, and (somewhat at odds with the ecological need for biodegradability) biostability should be considered in the design and functionalization of such materials. Several representative designs of SHAF materials, both with and without a direct aim toward bioapplications, are presented below in view of such potential applications.

3.1. Protective Coatings

SHAF coatings can be applied onto many surfaces to work as protecting layer to prevent the deposition of many foulants such as biomaterials, ice or oil, leading to long-term antibacterial, anti-icing,[80,89] antifogging,[90] and anticorrosion[91] properties. A typical example would be to use SHAF materials on boat surfaces to prevent hull fouling[92] as caused by marine microorganisms. Furthermore, typically the protecting function of coatings will be reduced upon damage due to prolonged exposure to the often harsh environment. The self-healing properties of SHAF materials can therefore not only extend the service time of the materials, but also prevent or strongly reduce the damaged area to be fouled or corroded.

As an example, Choi and co-workers fabricated an anodic aluminum oxide (AAO) layer on an aluminum substrate, which contains high-aspect-ratio dead-end nanopores infused by oil through a solvent exchange method. This structure was coated with a hydrophobic Teflon layer, and subsequently impregnated by the oil, to establish a highly robust and stable nonwetting surface against water on the AAO surface. The Teflon-coated hydrophobic nanopores were fully and stably infused by oil, which prevents corrosive aqueous media from penetrating into the pores, thereby further enhancing the corrosion resistance of aluminum. The infused liquid oil can wick into damaged sites such as cracks in the AAO layer, thereby further reducing the exposure of the aluminum surface to the outer environment, and thus minimizing corrosion.[50] Somewhat analogously, Li and co-workers utilized electroplating combined with a chemical replacement reaction to fabricate a Krytox 100-infused porous Zn–Ni–Co SLIPS, which exhibited an excellent anticorrosion performance, even after immersion in NaCl solution, and self-healing.[52] Moreover, the lubricant in the pores can walk into any destroyed domains and repair the surface, and thus repaired materials demonstrated a good self-healing and anticorrosion performance.

3.2. Oil/Water Separation

Marine resources are quite vulnerable to anthropogenic disasters such as oil leakage and oil spill accidents, which as such have become one of the top environmental concerns. Therefore, oil/water separation has become an emerging and fast rising topic in both academic and industrial research. Wettable materials with obviously opposite affinities toward oil and water are considered to be the most promising materials for achieving high efficiency oil/water separation.[93] Such materials are typically placed into two categories in view of the approaches that were utilized for oil/water separation. One kind is formed by filtration materials such as textiles, membranes, meshes and so on, while the other kind is that of absorption materials, including sponges, aerogels and particles. As a typical example, Feng et al. demonstrated the use a superamphiphobic material for oil/water separations.[94] Subsequently, many innovative materials with special wettable properties have been developed to be used for oil/water separation.[95] Depositing SHAF materials onto porous materials for oil/water separation can improve the separation efficiency, taking the oil as the foulant here, and prolong the lifetime of the materials.[96]

Guo et al. prepared superhydrophobic fabrics via an in–situ growth method to fabricate hierarchical flower-like MnO_2 nanoparticles on cotton fabric surface and subsequent stearic acid modification, exhibiting multifunctional self-healing, self-cleaning, oil/water separating and wear-resisting behavior (**Figure 15**A).[96a] After an air-plasma treatment, the originally superhydrophobic fabric displayed a fully hydrophilic performance with a water CA of 0°, as shown in Figure 15B. Interestingly, the superhydrophobicity could be recovered (water CA 153°) at least eight times, when the plasma-damaged fabric was heated to 130 °C for 10 min. Obvious oil–water separation behavior can be seen without external intervention as manifested by the oil quickly passing through the MnO_2@fabric and dropping into the conical flask, and successfully blocking the water to the vessel (Figure 15C). After five successive etching–heating cycles, the oil/water separation ability still maintains at 90%. This thus indicates that the reusable fabric still can regenerate the superhydrophobicity very well, while for water–oil separations, this contributes significantly to further steps in the field.

Liu and co-workers coated on polyethylene terephthalate (PET) fabrics with a self-healing silicon elastomer which was crosslinked via cobalt (Co)-based coordination bonding, exhibiting hydrophobic properties as revealed by a CA of >140°, a high oil/water separation efficiency of around 99%, high durability (even at extremely low temperatures) as well as an ultrafast self-healing behavior at room temperature (Figure 15D).[97] Oil/water separation experiments shows that water permeated through the Co-PDMS@PET fabrics that is damaged by immersing into liquid nitrogen due to the decrease of the surface hydrophobicity and the oil/water separation performance deteriorated severely. A 98% separation efficiency for the chloroform/water mixture was obtained after the damaged fabric

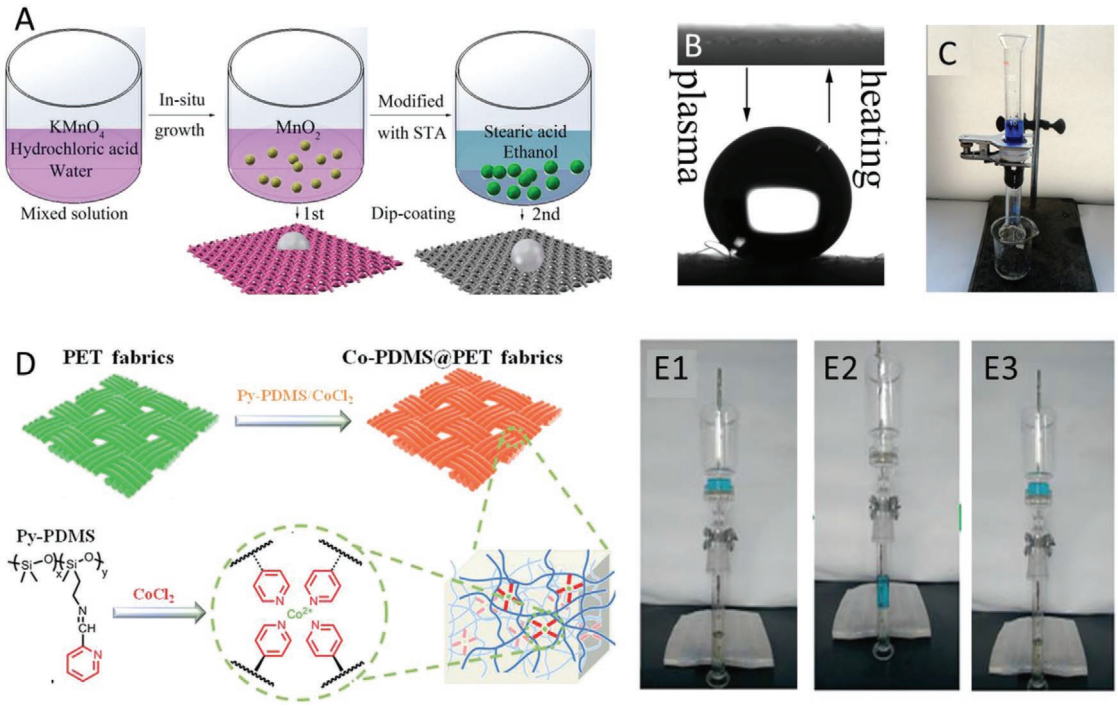

Figure 15. A) Fabrication process of MnO_2@cotton fabric. B) Optical images showing repair of superhydrophobicity through heat stimulation. C) Photograph (water is filtered out, while purpose-colored oil is left) showing the oil/water separation process with the superhydrophobic MnO2@ fabric. Reproduced with permission.[96a] Copyright 2017, Elsevier. D) Preparation route of the Co-PDMS@PET fabric. Photographs (water is filtered out, while purpose-colored oil is left) showing the oil/water separation process with the freshly prepared E1), damaged E2), and repaired E3) Co-PDMS@ PET fabric. Reproduced with permission.[97] Copyright 2018, Royal Society of Chemistry.

was repaired at room temperature for 10 min, which indicates that the oil/water separation performance could be quickly recovered (Figure 15E).

3.3. Injectable and Implantable Hydrogels

Injectable hydrogels are emerging as promising candidates for biomedical applications such as drug delivery, due to their biocompatibility, ease of administration, and minimally invasive character owing to their high resemblance with natural extracellular matrices.[98] However, proteins or microorganisms can easily adhere to implanted hydrogels and form biofouling films, which will block the circulation of loaded biomolecules and induce an immune response or inflammation. A common way to overcome this challenging issue is to impart the developed hydrogels with antifouling or antibacterial properties to reduce the accumulation of biofouling films on their surfaces.[99] Implanted hydrogels inevitably result in certain deformation or damage of the hydrogels due to suffering from constant external mechanical forces after injection. Once disruption takes place in vivo, body fluids will intrude and simultaneously introduce nutrients and microorganisms to build up detrimental biofoulings, while additionally speeding up the delivery of the embedded drugs to the surrounding tissue. Both the inflammatory response and the uncontrolled delivery rate will hamper any use. In such real-life circumstances, a hydrogel possessing autonomous healing capabilities under physiological conditions upon damage will be of great significance, because the maintained integrity of the shape and structure of the gels, prevention of a burst release of the loaded biomolecules and overall a strongly enhanced delivery control and efficiency.[100] To meet with different demands in dynamic biomedical processes, multifunctional hydrogels integrating biologically relevant features—such as in situ gelation capabilities and injectability to facilitate operation; antimicrobial and antifouling properties to inhibit bacterial growth and biofilm accumulation; and self-healing properties to ensure structural and functional integrity—would be of significant potential for bioengineering applications.

Based on the desired dynamic chemical/physical interactions, many different kinds of injectable or implantable SHAF hydrogels can be fabricated.[103] Zeng's group reported an injectable hydrogel based on self-organization of an ABA triblock polymer [poly[(*N*-isopropylacrylamide)-*co*-(*N*-3,4-dihydroxyphenethyl acrylamide)]-*b*-poly(ethylene oxide)-*b*-poly[(*N*-isopropylacrylamide)-*co*-(*N*-3,4-dihydroxyphenethylacrylamide)], short name: DNODN; **Figure 16**A] with rapid self-healing properties based on catechol-mediated hydrogen bonding and aromatic interactions and with anti-biofouling capability (Figure 16B).[101] As could be seen from the rheology results, the heating process increased storage modulus (G') significantly faster than loss modulus (G''), and became much larger than G'' at higher temperature, indicating a gel-like property. The crossover between G' and G'' at 16 °C was considered to be the

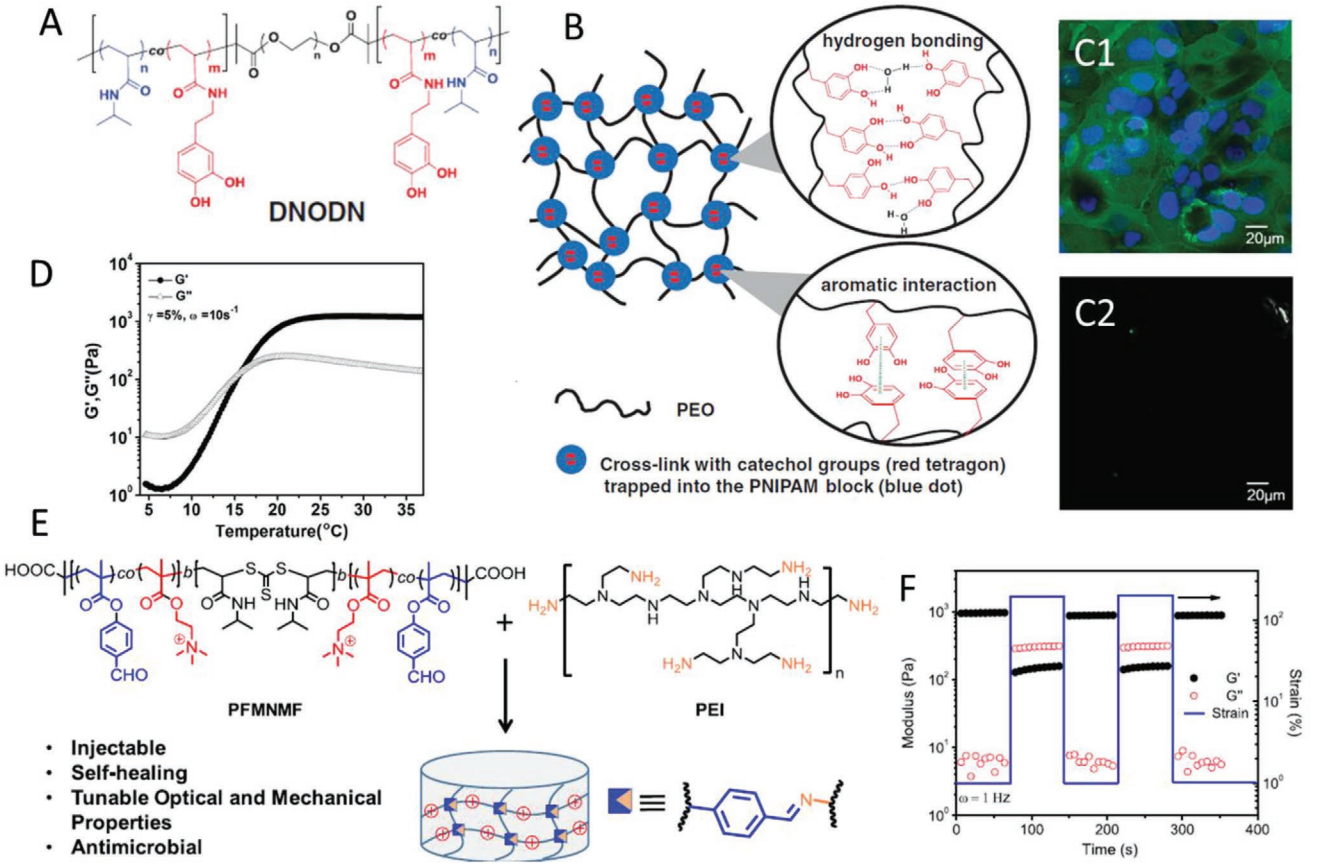

Figure 16. A) Chemical structure of the ABA tri-block copolymer DNODN. B) Proposed structure of the DNODN hydrogel. Fluorescence microscopy images of uncoated C1) and hydrogel-coated C2) microwell dishes after exposure to Caco-2 cells for 48 h. D) Temperature-responsive storage (*G′*) and loss (*G″*) modulus changes of a 10 wt% DNODN hydrogel. Reproduced with permission.[101] Copyright 2015, Wiley-VCH. E) A "PFMNMF + PEI"-based injectable self-healing hydrogel with tunable optical, mechanical, and antimicrobial properties. F) Dynamic cyclic strain sweep measurements of Gel-9.5% at 25 °C. Reproduced with permission.[102] Copyright 2019, American Chemical Society.

sol–gel transition temperature (Figure 16D). Antifouling studies showed that a dense cell layer was formed at the bottom of the microwell dishes, indicating strong fouling due to the Caco-2 cells adhesion. In contrast, DNODN hydrogel-coated microwell dishes showed an excellent resistance to such cell adhesion, which could be attributed to the presence of a major component PEO (Figure 16C1,C2). The thermally induced shearing-thinning behavior makes the hydrogel injectable in vivo at body temperature. This hydrogel can effectively prevent the formation of biofilms due to its excellent anti-biofouling properties. In a similar study, this group developed another injectable ABA triblock copolymer hydrogel with excellent self-healing character, and with tunable mechanical, optical and antimicrobial properties (molecular structure shown in Figure 16E). The self-healing capability of this hydrogel was confirmed by rheology tests (Figure 16F). Quantitative force measurements by a surface forces apparatus provided molecular insights into the self-healing mechanism that was realized using the Schiff base reaction. The hydrogel also possessed multiple sol–gel transitions when subjected to pH change, and can effectively prevent the growth of both Gram-negative and Gram-positive bacteria (*E. coli* and *S. aureus*), while showing low cytotoxicity to both fibroblast and cancer cells (MRC-5 and HeLa).[102]

Other dynamic covalent chemistry approaches have also been invoked. Antifouling and antibacterial hydrogel coatings made of (poly(ethyleneglycol)methyl ether methacrylate (PEGMA), *N*-hydroxyethyl acrylamide (HEAA) and 2-(methacryloyloxy)-ethyl trimethylammonium chloride (META)) and a disulfide-containing crosslinker bis(2-methacryloyl)-oxyethyl disulfide with self-healing properties based on a dynamic disulfide exchange reaction were reported by Wang and co-workers.[104] Liu and co-workers developed a supramolecular polymer hydrogel through the copolymerization of *N*-acryloyl glycinamide (NAGA) and carboxybetaine acrylamide (CBAA). This polymer displayed excellent SHAF properties due to the multiple hydrogen-bonding interactions between the double amide bonds and the ionic interaction between the carboxybetaine groups.[105] Based on the dynamic covalent imine bond, Ma and co-workers fabricated injectable bioactive wound dressings that are made of conductive hydrogels with excellent self-healing and antioxidant character. This hydrogel dressing could effectively accelerate the wound healing process, as shown in a full-thickness skin defect model.[26b] Based on the dynamic nature of the Ag-S coordination bond, and the bacteria-killing activity of Ag^+, Deng et al. developed a self-healing, injectable and antibacterial hydrogel that could efficiently repair diabetic

skin wounds with low bacterial infection and enhance antigenic activity.[106]

Dynamic chemistry plays a very important role in turning generic SHAF materials into tailor-made injectable hydrogels, which can induce sol–gel transition and shearing-thinning behavior to enable smooth injecting and fast gelation. Non-covalent bonds or pH-sensitive dynamic covalent bonds are good choices to design this kind of materials due to their low dissociation energies of activation $\Delta H^{\neq}$ under physiological conditions. The reversible cleavage and formation of the dynamic bond then endows the materials with shear-thinning properties, leading to fast gelation after injection. It is difficult to achieve such shear-thinning property via most dynamic covalent bonds, due to their relative high bonding energy, high value of $\Delta H^{\neq}$. Kinetics barriers are too low would also hamper effective use, as the reversible reaction should be fast enough to enable the gelation after injection, to avoid the flowing of the injectable materials.

As we can see from this, admittedly limited, selection of examples, these kinds of injectable hydrogels are normally used in vivo, making their biocompatibility and eventually: biodegradation, highly important. The antifouling properties of the injectable hydrogels usually come from zwitterionic or PEG groups, as low-surface energy materials are not suitable in this application. In order to further increase the antibacterial properties of these materials, polymer segments containing quaternary ammonium salt groups will likely be useful. Along the same lines, integrating other antibacterial reagents such as silver nanoparticles or carbon dots into such injectable hydrogels could be a future research topic. The dispersion of these inorganic nanoparticles in the hydrogels and their biocompatibility, biodegradation and the interaction with the hydrogels should also be considered.

4. Outlook and Perspective

In this review, we have presented some recent developments of SHAF materials and discussed healing and antifouling mechanisms and properties of these materials. Although many different kinds of antifouling materials with excellent durability have been developed, there is still ample room to develop novel materials with nice antifouling properties relying on innovative concepts. In the various chapters above, several specific conclusions were already specified, which might point to future research goals. Such recommendations can also be made more generic: we believe that more attention should be paid to the following aspects when developing such materials. The as-discussed self-healing antifouling systems in this review article are typically based on relatively simple modes of foulant adsorption. However, fouling as happening in realistic systems is often highly complicated, with different limiting factors during the various stages of fouling. The currently accepted mechanisms and characterization methods to explain and quantify fouling, respectively, can be a guide for designing antifouling materials, but will likely sometimes still fail, as a deeper understanding of the multiscale fouling process is still really needed. Based on the damage style and degree, we characterized the healing efficiency in different ways. Simple, one type of damage-only approaches (disappearance of a scratch, recovery of surface roughness and hydrophobicity and recombining of two cut-off samples) are the three main methods to evaluate the healing efficiency. However, antifouling materials are often used in environments than will produce all sort of defects simultaneously. In addition, the degree of damage can often not be anticipated, which makes the development of self-healing materials that can repair any kind of damage, like those outlined in category III, of vital importance.

Several aspects might be especially promising in such novel science. 1) Novel functional moieties. Rather than only mix well-known components in novel manners to obtain interesting properties, the development of new kinds of antifouling materials based on molecular design will be needed to help deepen the understanding of the antifouling process. For example, Jiang and co-workers reported a new class of trimethylamine N-oxide based zwitterionic polymer materials (PTMAO) which displayed an ultrahigh protein-repellence in undiluted blood serum.[107] Furthermore, PTMAO exhibited minimal immunogenicity and extended circulation after being conjugated to highly immunogenic protein carriers. Molecular dynamics simulations illustrated that the strong hydrogen bonding with water and a continuous hydration layer around the PTMAO headgroups could be responsible for its superhydrophilic and antifouling properties. Whereas no single functionality will display a "one-size-fits-all"-quality, novel synthetic work is essential to further both understanding and development of SHAF materials. 2) Quantitative characterization of the degree of fouling. Such characterization is actually still a challenge. Some optical methods such as microscopic observations and reflectometry are fine choices, but they are only suitable for ultraflat surfaces. 3) Local characterization of antifouling property of the original, damaged, and repair areas. We recommend the use of fluorescence-labeled protein as model fouling materials, and microscopy to observe the fluorescence differentiation between the damaged and repaired area. The reason for this recommendation is that this is a stringent test for repair, as, e.g., recovery of superhydrophobicity often is much easier to achieve than anti-biofouling. 4) Multifoulant studies. Many of the as-developed antifouling materials are only highly repellent for one special kind of foulants. Developing a more comprehensive set of antifouling materials will be necessary to meet with real-life application requirements. For example, zwitterionic materials were confirmed to possess excellent anti-biofouling materials, especially a high repellence for protein. However, upon use of these materials for ocean-based marine applications, the observed antifouling property is not yet satisfactory, likely due to the complex environment and many different kinds of foulants (ranging from individual proteins and oil components to mussels and barnacles) in the sea. 5) Repair under physiological conditions. Developing coatings that can be repaired under physiologically relevant conditions, i.e., salt-containing aqueous media, is very interesting, as it is relevant to both injectable hydrogel studies, as well as to marine studies. 6) Increase mechanical stability, for example by novel dynamic covalent chemistries. The self-healing function also endows the materials with dynamic properties that might result in a stability balance problem. As SHAF materials sometimes are used in harsh environments,

significant efforts are needed be to simultaneously guarantee both excellent self-healing and high stability. 7) Multiscale studies. Fouling starts with the addition of a single molecule. The addition of subsequent foulants is often influenced by the degree of fouling already present. Therefore, following the fouling process in much detail over time and in space is needed to deepen our understanding. 8) Avoiding fluorinated compounds. Although low-surface-energy fluorinated materials display excellent SHAF properties, the prolonged use of polyfluorinated alkyl chains is ecologically unacceptable. For environmentally acceptable solutions, it is thus imperative that future studies avoid the use these materials, and focus on fluorine-free or short-chain fluorinated compounds (which are not environmentally hazardous, C_3F_7 and smaller) without sacrificing the SHAF properties.

Last but not the least, 9) 3D printing. Fabricating multifunctional devices by 3D printing SHAF materials will be a hot topic in this field in the future study. A delicate balance between the flow property of polymer inks and structural fidelity of printed objects can be realized by incorporating dynamic chemical bonds into the polymer inks. Dynamic chemistry endows the polymer inks with shear-thinning and self-healing properties due to the reversible cleavage and formation of chemical bonds, which leads to smooth 3D printing process and high-resolution printed objects with well-defined features. The products fabricated via 3D printing can still possess both self-healing and antifouling properties. Moreover, the structure and architecture can be tailor-made through 3D printing with the aid of computer simulation. Many potential applications such as oil/water separation[108] and artificial organ studies are within view, and we expect significant potential for 3D-printing of SHAF materials in the future.

In summary, the fabrication of durable SHAF materials has opened up a great field, in which there is more than enough room for further explorations. Molecular design and materials processing should be more focused to develop novel SHAF materials and achieve their function. We hope that our personal, and undoubtedly biased and limited, opinions will help readers quickly catch hold of the recent progress in SHAF materials and develop improved fabrication methods and novel materials for fundamental investigations and practical applications in the near future.

Acknowledgements

This work was financially supported by the National Key R&D Program of China (2017YFE0111500), the National Natural Science Foundation of China (Grants No. 51703143 to Z.W. and 21871208 to H.Z.), the International Cooperation Project of Sichuan Province (2019YFH0135), the Fundamental Research Funds for the Central University (YJ201707), the 973 National Basic Research Program of China (No. 2015CB856500 to H.Z.), the Tianjin City Thousand Talents Program (to H.Z.), and Wageningen University.

Conflict of Interest

Luc Scheres is CEO of Surfix B.V., a company, cofounded by Zuilhof and Scheres in 2011, that focuses on nanocoatings.

Keywords

antifouling materials, oil/water separation, self-healing materials, self-replenishing surface, zwitterionic materials

Received: September 30, 2019
Revised: December 10, 2019
Published online: April 20, 2020

[1] C. M. Kirschner, A. B. Brennan, *Annu. Rev. Mater. Res.* **2012**, *42*, 211.
[2] B. Bansal, H. Muller-Steinhagen, X. D. Chen, *Heat Transfer Eng.* **2001**, *22*, 13.
[3] T. Stephenson, A. Kubis, M. Derakhshesh, M. Hazelton, C. Holt, P. Eaton, B. Newman, A. Hoff, M. Gray, D. Mitlin, *Energy Fuels* **2011**, *25*, 4540.
[4] M. K. Sarvothaman, K. S. Kim, B. Seale, P. M. Brodersen, G. C. Walker, A. R. Wheeler, *Adv. Funct. Mater.* **2015**, *25*, 506.
[5] G. D. Bixler, B. Bhushan, *Philos. Trans. R. Soc., A* **2012**, *370*, 2381.
[6] S. Shirazi, C. J. Lin, D. Chen, *Desalination* **2010**, *250*, 236.
[7] W. S. Ang, A. Tiraferri, K. L. Chen, M. Elimelech, *J. Membr. Sci.* **2011**, *376*, 196.
[8] a) X. N. Zhang, D. Brodus, V. Hollimon, H. M. Hu, *Chem. Cent. J.* **2017**, *11*, 12; b) U. Eduok, O. Faye, J. Szpunar, *Prog. Org. Coat.* **2017**, *111*, 124.
[9] a) Q. H. Sun, H. Q. Li, C. Y. Xian, Y. H. Yang, Y. X. Song, P. H. Cong, *Appl. Surf. Sci.* **2015**, *344*, 17; b) Y. Zhang, Y. H. Qi, Z. P. Zhang, G. Y. Sun, *J. Coat. Technol. Res.* **2015**, *12*, 215.
[10] M. Rosso, A. T. Nguyen, E. de Jong, J. Baggerman, J. M. J. Paulusse, M. Giesbers, R. G. Fokkink, W. Norde, K. Schroen, C. J. M. van Rijn, H. Zuilhof, *ACS Appl. Mater. Interfaces* **2011**, *3*, 697.
[11] a) A. T. Nguyen, J. Baggerman, J. M. J. Paulusse, C. J. M. van Rijn, H. Zuilhof, *Langmuir* **2011**, *27*, 2587; b) J. B. Schlenoff, *Langmuir* **2014**, *30*, 9625; c) Z. Zhang, T. Chao, S. F. Chen, S. Y. Jiang, *Langmuir* **2006**, *22*, 10072; d) S. Y. Jiang, Z. Q. Cao, *Adv. Mater.* **2010**, *22*, 920; e) Q. Shao, S. Y. Jiang, *Adv. Mater.* **2015**, *27*, 15; f) S. C. Lange, E. van Andel, M. M. J. Smulders, H. Zuilhof, *Langmuir* **2016**, *32*, 10199.
[12] Z. H. Wang, S. P. Pujari, B. van Lagen, M. M. J. Smulders, H. Zuilhof, *Adv. Mater. Interfaces* **2016**, *3*, 1500514.
[13] a) Z. H. Wang, H. Zuilhof, *J. Mater. Chem. A* **2016**, *4*, 2408; b) Z. H. Wang, H. Zuilhof, *Langmuir* **2016**, *32*, 6571; c) Z. H. Wang, H. Zuilhof, *Langmuir* **2016**, *32*, 6310.
[14] a) M. R. Detty, R. Ciriminna, F. V. Bright, M. Pagliaro, *Acc. Chem. Res.* **2014**, *47*, 678; b) J. A. Callow, M. E. Callow, *Nat. Commun.* **2011**, *2*, 244.
[15] a) T. S. Wong, S. H. Kang, S. K. Y. Tang, E. J. Smythe, B. D. Hatton, A. Grinthal, J. Aizenberg, *Nature* **2011**, *477*, 443; b) J. S. Li, E. Ueda, D. Paulssen, P. A. Levkin, *Adv. Funct. Mater.* **2019**, *29*, 13; c) P. Kim, T. S. Wong, J. Alvarenga, M. J. Kreder, W. E. Adorno-Martinez, J. Aizenberg, *ACS Nano* **2012**, *6*, 6569; d) A. K. Epstein, T. S. Wong, R. A. Belisle, E. M. Boggs, J. Aizenberg, *Proc. Natl. Acad. Sci. USA* **2012**, *109*, 13182; e) L. L. Xiao, J. S. Li, S. Mieszkin, A. Di Fino, A. S. Clare, M. E. Callow, J. A. Callow, M. Grunze, A. Rosenhahn, P. A. Levkin, *ACS Appl. Mater. Interfaces* **2013**, *5*, 10074; f) C. Howell, A. Grinthal, S. Sunny, M. Aizenberg, J. Aizenberg, *Adv. Mater.* **2018**, *30*, 1802724; g) Z. Ashrafi, L. Lucia, W. Krause, *ACS Appl. Mater. Interfaces* **2019**, *11*, 21275.
[16] A. Worz, B. Berchtold, K. Moosmann, O. Prucker, J. Ruhe, *J. Mater. Chem.* **2012**, *22*, 19547.
[17] a) R. F. Diegelmann, M. C. Evans, *Front. Biosci.* **2004**, *9*, 283; b) R. Han, K. P. Campbell, *Curr. Opin. Cell Biol.* **2007**, *19*, 409.
[18] a) B. Ghosh, M. W. Urban, *Science* **2009**, *323*, 1458; b) M. W. Urban, D. Davydovich, Y. Yang, T. Demir, Y. Z. Zhang,

L. Casabianca, *Science* **2018**, *362*, 220; c) Y. Yang, D. Davydovich, C. C. Hornat, X. L. Liu, M. W. Urban, *Chem* **2018**, *4*, 1928; d) Y. Yang, M. W. Urban, *Chem. Soc. Rev.* **2013**, *42*, 7446; e) Y. Yang, X. C. Ding, M. W. Urban, *Prog. Polym. Sci.* **2015**, *49–50*, 34.

[19] a) Z. H. Wang, M. W. Urban, *Polym. Chem.* **2013**, *4*, 4897; b) Z. H. Wang, Y. Yang, R. Burtovyy, I. Luzinov, M. W. Urban, *J. Mater. Chem. A* **2014**, *2*, 15527; c) Z. H. Wang, S. Gangarapu, J. Escorihuela, G. X. Fei, H. Zuilhof, H. S. Xia, *J. Mater. Chem. A* **2019**, *7*, 15933; d) Z. Wang, X. Lu, S. Sun, C. Yu, H. Xia, *J. Mater. Chem. B* **2019**, *7*, 4876; e) L. R. Tian, L. Yang, Z. H. Wang, H. S. Xia, *Acta Polym. Sin.* **2019**, *50*, 527; f) D. H. Fu, W. L. Pu, Z. H. Wang, X. L. Lu, S. J. Sun, C. J. Yu, H. S. Xia, *J. Mater. Chem. A* **2018**, *6*, 18154; g) W. L. Pu, D. H. Fu, Z. H. Wang, X. P. Gan, X. L. Lu, L. Yang, H. S. Xia, *Adv. Sci.* **2018**, *5*, 1800101; h) L. Yang, X. L. Lu, Z. H. Wang, H. S. Xia, *Polym. Chem.* **2018**, *9*, 2166; i) Z. H. Wang, C. Xie, C. J. Yu, G. X. Fei, Z. H. Wang, H. S. Xia, *Macromol. Rapid Commun.* **2018**, *39*, 1800635; j) J. Zhao, R. Xu, G. X. Luo, J. Wu, H. S. Xia, *J. Mater. Chem. B* **2016**, *4*, 982; k) X. L. Lu, G. X. Fei, H. S. Xia, Y. Zhao, *J. Mater. Chem. A* **2014**, *2*, 16051; l) J. Zhao, R. Xu, G. X. Luo, J. Wu, H. S. Xia, *Polym. Chem.* **2016**, *7*, 7278.

[20] S. R. White, N. R. Sottos, P. H. Geubelle, J. S. Moore, M. R. Kessler, S. R. Sriram, E. N. Brown, S. Viswanathan, *Nature* **2001**, *409*, 794.

[21] a) M. Q. Zhang, M. Z. Rong, *Polym. Chem.* **2013**, *4*, 4878; b) M. Enke, D. Dohler, S. Bode, W. H. Binder, M. D. Hager, U. S. Schubert, *Self-Healing Materials*, Vol. *273* (Eds: M. D. Hager, S. VanDerZwaag, U. S. Schubert), Springer-Verlag, Berlin **2016**, p. 59.

[22] X. K. D. Hillewaere, F. E. Du Prez, *Prog. Polym. Sci.* **2015**, *49–50*, 121.

[23] a) A. Stankiewicz, I. Szczygiel, B. Szczygiel, *J. Mater. Sci.* **2013**, *48*, 8041; b) H. C. Qian, D. K. Xu, C. W. Du, D. W. Zhang, X. G. Li, L. Y. Huang, L. P. Deng, Y. C. Tu, J. M. C. Mol, H. A. Terryn, *J. Mater. Chem. A* **2017**, *5*, 2355.

[24] a) H. Zhou, H. X. Wang, H. T. Niu, A. Gestos, T. Lin, *Adv. Funct. Mater.* **2013**, *23*, 1664; b) H. Zhou, H. X. Wang, H. T. Niu, Y. Zhao, Z. G. Xu, T. Lin, *Adv. Funct. Mater.* **2017**, *27*, 8.

[25] a) Y. Li, S. S. Chen, M. C. Wu, J. Q. Sun, *Adv. Mater.* **2012**, *24*, 4578; b) K. A. Williams, A. J. Boydston, C. W. Bielawski, *J. R. Soc., Interface* **2007**, *4*, 359; c) B. C. K. Tee, C. Wang, R. Allen, Z. N. Bao, *Nat. Nanotechnol.* **2012**, *7*, 825.

[26] a) X. Wang, Y. Wang, S. Bi, Y. G. Wang, X. G. Chen, L. Y. Qiu, J. Q. Sun, *Adv. Funct. Mater.* **2014**, *24*, 403; b) X. Zhao, H. Wu, B. L. Guo, R. N. Dong, Y. S. Qiu, P. X. Ma, *Biomaterials* **2017**, *122*, 34.

[27] S. Liu, W. W. Guo, *Adv. Funct. Mater.* **2018**, *28*, 25.

[28] a) M. Diba, S. Spaans, K. Ning, B. D. Ippel, F. Yang, B. Loomans, P. Y. W. Dankers, S. C. G. Leeuwenburgh, *Adv. Mater. Interfaces* **2018**, *5*, 1800118; b) C. Esteves, *Adv. Mater. Interfaces* **2018**, *5*, 1800293; c) B. D. Ippel, P. Y. W. Dankers, *Adv. Healthcare Mater.* **2018**, *7*, 1700505.

[29] a) S. van der Zwaag, A. M. Grande, W. Post, S. J. Garcia, T. C. Bor, *Mater. Sci. Technol.* **2014**, *30*, 1633; b) S. J. Garcia, H. R. Fischer, S. van der Zwaag, *Prog. Org. Coat.* **2011**, *72*, 211; c) J. B. Limin Wu, *Functional Polymer Coatings: Principles, Methods, and Applications*, Wiley, Hoboken **2015**, Ch. 4, p. 133; d) G. de With, *Polymer Coatings: A Guide to Chemistry, Characterization, and Selected Applications*, Wiley-VCH, Weinheim, Germany **2018**.

[30] a) L. D. Chambers, K. R. Stokes, F. C. Walsh, R. J. K. Wood, *Surf. Coat. Technol.* **2006**, *201*, 3642; b) L. Delauney, C. Compere, M. Lehaitre, *Ocean Sci.* **2010**, *6*, 503; c) J. E. Gittens, T. J. Smith, R. Suleiman, R. Akid, *Biotechnol. Adv.* **2013**, *31*, 1738; d) A. G. Nurioglu, A. C. C. Esteves, G. de With, *J. Mater. Chem. B* **2015**, *3*, 6547.

[31] T. Dikic, W. Ming, R. van Benthem, A. C. C. Esteves, G. de With, *Adv. Mater.* **2012**, *24*, 3701.

[32] a) X. Zhang, F. Shi, J. Niu, Y. G. Jiang, Z. Q. Wang, *J. Mater. Chem.* **2008**, *18*, 621; b) M. L. Ma, R. M. Hill, *Curr. Opin. Colloid Interface Sci.* **2006**, *11*, 193.

[33] a) R. Furstner, W. Barthlott, C. Neinhuis, P. Walzel, *Langmuir* **2005**, *21*, 956; b) X. J. Feng, L. Jiang, *Adv. Mater.* **2006**, *18*, 3063.

[34] A. C. C. Esteves, Y. Luo, M. W. P. van de Put, C. C. M. Carcouet, G. de With, *Adv. Funct. Mater.* **2014**, *24*, 986.

[35] K. Lyakhova, A. C. C. Esteves, M. W. P. van de Put, L. G. J. van der Ven, R. van Benthem, G. de With, *Adv. Mater. Interfaces* **2014**, *1*, 1400053.

[36] H. Zhang, C. P. Hou, L. X. Song, Y. Ma, Z. Ali, J. W. Gu, B. L. Zhang, H. P. Zhang, Q. Y. Zhang, *Chem. Eng. J.* **2018**, *334*, 598.

[37] Y. Li, L. Li, J. Q. Sun, *Angew. Chem., Int. Ed.* **2010**, *49*, 6129.

[38] a) S. S. Chen, X. Li, Y. Li, J. Q. Sun, *ACS Nano* **2015**, *9*, 4070; b) C. H. Xue, J. Z. Ma, *J. Mater. Chem. A* **2013**, *1*, 4146; c) T. Verho, C. Bower, P. Andrew, S. Franssila, O. Ikkala, R. H. A. Ras, *Adv. Mater.* **2011**, *23*, 673; d) Y. Lee, E. A. You, Y. G. Ha, *Appl. Surf. Sci.* **2018**, *445*, 368; e) K. L. Chen, K. Gu, S. Y. Qiang, C. X. Wang, *RSC Adv.* **2017**, *7*, 543; f) Y. Li, Z. Z. Zhang, M. K. Wang, X. H. Men, Q. J. Xue, *J. Mater. Chem. A* **2017**, *5*, 20277.

[39] X. S. Jing, Z. G. Guo, *J. Mater. Chem. A* **2018**, *6*, 16731.

[40] H. X. Wang, Y. H. Xue, J. Ding, L. F. Feng, X. G. Wang, T. Lin, *Angew. Chem., Int. Ed.* **2011**, *50*, 11433.

[41] R. R. Carvalho, S. P. Pujari, E. X. Vrouwe, H. Zuilhof, *ACS Appl. Mater. Interfaces* **2017**, *9*, 16644.

[42] a) H. D. Wang, H. Zhou, A. Gestos, J. Fang, T. Lin, *ACS Appl. Mater. Interfaces* **2013**, *5*, 10221; b) B. C. Li, J. P. Zhang, *Chem. Commun.* **2016**, *52*, 2744; c) X. Li, Y. Li, T. T. Guan, F. C. Xu, J. Q. Sun, *ACS Appl. Mater. Interfaces* **2018**, *10*, 12042; d) H. Zhang, J. J. Tan, Y. B. Liu, C. P. Hou, Y. Ma, J. W. Gu, B. L. Zhang, H. P. Zhang, Q. Y. Zhang, *Mater. Des.* **2017**, *135*, 16; e) H. Zhang, Y. B. Liu, C. P. Hou, Y. Ma, B. L. Zhang, H. P. Zhang, Q. Y. Zhang, *Surf. Coat. Technol.* **2017**, *331*, 97; f) X. L. Wang, X. J. Liu, F. Zhou, W. M. Liu, *Chem. Commun.* **2011**, *47*, 2324.

[43] H. Zhou, H. X. Wang, H. T. Niu, T. Lin, *Adv. Mater. Interfaces* **2018**, *5*, 24.

[44] H. Ye, L. Q. Zhu, W. P. Li, H. C. Liu, H. N. Chen, *ACS Appl. Mater. Interfaces* **2017**, *9*, 858.

[45] Y. R. Wang, W. Q. Yan, M. Frey, M. V. del Blanco, M. Schubert, M. Adobes-Vidal, E. Cabane, *Adv. Sustainable Syst.* **2019**, *3*, 12.

[46] Y. H. Liu, Z. L. Liu, Y. P. Liu, H. Y. Hu, Y. Li, P. X. Yan, B. Yu, F. Zhou, *Small* **2015**, *11*, 426.

[47] a) N. MacCallum, C. Howell, P. Kim, D. Sun, R. Friedlander, J. Ranisau, O. Ahanotu, J. J. Lin, A. Vena, B. Hatton, T. S. Wong, J. Aizenberg, *ACS Biomater. Sci. Eng.* **2015**, *1*, 43; b) X. T. Zhu, J. W. Lu, X. M. Li, B. Wang, Y. M. Song, X. Miao, Z. J. Wang, G. N. Ren, *Ind. Eng. Chem. Res.* **2019**, *58*, 8148.

[48] C. Howell, T. L. Vu, J. J. Lin, S. Kolle, N. Juthani, E. Watson, J. C. Weaver, J. Alvarenga, J. Aizenberg, *ACS Appl. Mater. Interfaces* **2014**, *6*, 13299.

[49] P. F. Zhang, H. W. Chen, L. W. Zhang, Y. Zhang, D. Y. Zhang, L. Jiang, *J. Mater. Chem. A* **2016**, *4*, 12212.

[50] J. Lee, S. Shin, Y. H. Jiang, C. Jeong, H. A. Stone, C. H. Choi, *Adv. Funct. Mater.* **2017**, *27*, 11.

[51] X. Yao, Y. H. Hu, A. Grinthal, T. S. Wong, L. Mahadevan, J. Aizenberg, *Nat. Mater.* **2013**, *12*, 529.

[52] T. F. Xiang, M. Zhang, H. R. Sadig, Z. C. Li, M. X. Zhang, C. D. Dong, L. Yang, W. M. Chan, C. Li, *Chem. Eng. J.* **2018**, *345*, 147.

[53] Q. Wei, C. Schlaich, S. Prevost, A. Schulz, C. Bottcher, M. Gradzielski, Z. H. Qi, R. Haag, C. A. Schalley, *Adv. Mater.* **2014**, *26*, 7358.

[54] L. Yu, G. Y. Chen, H. L. Xu, X. K. Liu, *ACS Nano* **2016**, *10*, 1076.
[55] Q. Q. Rao, A. Li, J. W. Zhang, J. X. Jiang, Q. H. Zhang, X. L. Zhan, F. Q. Chen, *J. Mater. Chem. A* **2019**, *7*, 2172.
[56] B. Shang, M. Chen, L. M. Wu, *ACS Appl. Mater. Interfaces* **2018**, *10*, 31777.
[57] X. Yao, S. W. Wu, L. Chen, J. Ju, Z. D. Gu, M. J. Liu, J. J. Wang, L. Jiang, *Angew. Chem., Int. Ed.* **2015**, *54*, 8975.
[58] H. Zhang, P. Wang, D. Zhang, *Colloids Surf. A* **2018**, *538*, 140.
[59] J. Y. Lv, X. Yao, Y. M. Zheng, J. J. Wang, L. Jiang, *Adv. Mater.* **2017**, *29*, 1703032.
[60] J. X. Cui, D. Daniel, A. Grinthal, K. X. Lin, J. Aizenberg, *Nat. Mater.* **2015**, *14*, 790.
[61] H. X. Zhao, Q. Q. Sun, X. Deng, J. X. Cui, *Adv. Mater.* **2018**, *30*, 6.
[62] Y. L. Wang, X. Yao, S. W. Wu, Q. Y. Li, J. Y. Lv, J. J. Wang, L. Jiang, *Adv. Mater.* **2017**, *29*, 7.
[63] X. F. Meng, Z. B. Wang, L. L. Wang, L. P. Heng, L. Jiang, *J. Mater. Chem. A* **2018**, *6*, 16355.
[64] A. Sandhu, O. J. Walker, A. Nistal, K. L. Choy, A. J. Clancy, *Chem. Commun.* **2019**, *55*, 3215.
[65] H. Kuroki, I. Tokarev, D. Nykypanchuk, E. Zhulina, S. Minko, *Adv. Funct. Mater.* **2013**, *23*, 4593.
[66] K. L. Chen, S. X. Zhou, L. M. Wu, *ACS Nano* **2016**, *10*, 1386.
[67] D. H. Wang, H. Y. Liu, J. L. Yang, S. X. Zhou, *ACS Appl. Mater. Interfaces* **2019**, *11*, 1353.
[68] K. L. Chen, S. X. Zhou, L. M. Wu, *RCS Adv.* **2015**, *5*, 104907.
[69] I. Jimenez-Pardo, L. G. J. van der Ven, R. van Benthem, G. de With, A. C. C. Esteves, *Coatings* **2018**, *8*, 184.
[70] W. S. Wang, R. A. Siegel, C. Wang, *ACS Biomater. Sci. Eng.* **2016**, *2*, 180.
[71] X. Wang, F. Liu, X. W. Zheng, J. Q. Sun, *Angew. Chem., Int. Ed.* **2011**, *50*, 11378.
[72] D. D. Chen, M. D. Wu, B. C. Li, K. F. Ren, Z. K. Cheng, J. Ji, Y. Li, J. Q. Sun, *Adv. Mater.* **2015**, *27*, 5882.
[73] X. P. Hao, W. H. Wang, Z. Q. Yang, L. F. Yue, H. Y. Sun, H. F. Wang, Z. H. Guo, F. Cheng, S. G. Chen, *Chem. Eng. J.* **2019**, *356*, 130.
[74] Z. H. Wang, E. van Andel, S. P. Pujari, H. H. Feng, J. A. Dijksman, M. M. J. Smulders, H. Zuilhof, *J. Mater. Chem. B* **2017**, *5*, 6728.
[75] Y. X. Li, T. Z. Pan, B. H. Ma, J. Q. Liu, J. Q. Sun, *ACS Appl. Mater. Interfaces* **2017**, *9*, 14429.
[76] J. L. Li, Y. Zhang, S. Zhang, M. Q. Liu, X. Li, T. Cai, *J. Mater. Chem. A* **2019**, *7*, 8167.
[77] W. X. Lei, X. C. Chen, M. Hu, H. Chang, H. Xu, K. F. Ren, J. Ji, *J. Mater. Chem. B* **2016**, *4*, 6358.
[78] Y. H. Zhang, L. Yuan, Q. B. Guan, G. Z. Liang, A. J. Gu, *J. Mater. Chem. A* **2017**, *5*, 16889.
[79] F. Li, Q. Q. Ye, Q. Gao, H. Chen, S. Q. Shi, W. R. Zhou, X. N. Li, C. L. Xia, J. Z. Li, *ACS Appl. Mater. Interfaces* **2019**, *11*, 16107.
[80] Y. Z. Zhuo, V. Hakonsen, Z. W. He, S. B. Xiao, J. Y. He, Z. L. Zhang, *ACS Appl. Mater. Interfaces* **2018**, *10*, 11972.
[81] C. Liu, C. F. Ma, Q. Y. Xie, G. Z. Zhang, *J. Mater. Chem. A* **2017**, *5*, 15855.
[82] Z. P. Ye, P. S. Zhang, J. H. Zhang, L. D. Deng, J. W. Zhang, C. G. Lin, R. W. Guo, A. J. Dong, *Prog. Org. Coat.* **2019**, *127*, 211.
[83] G. Wu, J. L. An, X. Z. Tang, Y. Xiang, J. L. Yang, *Adv. Funct. Mater.* **2014**, *24*, 6751.
[84] Z. H. Wang, G. X. Fei, H. S. Xia, H. Zuilhof, *J. Mater. Chem. B* **2018**, *6*, 6930.
[85] F. C. Xu, X. Li, D. H. Weng, Y. Li, J. Q. Sun, *J. Mater. Chem. A* **2019**, *7*, 2812.
[86] H. Zhang, Y. Z. Liang, P. Wang, D. Zhang, *Prog. Org. Coat.* **2019**, *132*, 132.
[87] S. Ramakrishna, K. S. S. Kumar, D. Mathew, C. P. R. Nair, *Sci. Rep.* **2015**, *5*, 11.
[88] B. Y. Jin, M. Z. Liu, Q. H. Zhang, X. L. Zhan, F. Q. Chen, *Langmuir* **2017**, *33*, 10340.
[89] a) T. Ghosh, N. Karak, *J. Colloid Interface Sci.* **2019**, *540*, 247; b) C. Urata, G. J. Dunderdale, M. W. England, A. Hozumi, *J. Mater. Chem. A* **2015**, *3*, 12626.
[90] F. C. Xu, X. Li, Y. Li, J. Q. Sun, *ACS Appl. Mater. Interfaces* **2017**, *9*, 27955.
[91] a) D. W. Li, H. Y. Wang, Y. Liu, D. S. Wei, Z. X. Zhao, *Chem. Eng. J.* **2019**, *367*, 169; b) N. Yang, Z. S. Wang, Z. Y. Zhu, S. C. Chen, G. Wu, *Ind. Eng. Chem. Res.* **2018**, *57*, 14517.
[92] a) M. Tribou, G. Swain, *Biofouling* **2010**, *26*, 47; b) M. P. Schultz, J. A. Bendick, E. R. Holm, W. M. Hertel, *Biofouling* **2011**, *27*, 87; c) S. Gollasch, *Biofouling* **2002**, *18*, 105.
[93] Q. L. Ma, H. F. Cheng, A. G. Fane, R. Wang, H. Zhang, *Small* **2016**, *12*, 2186.
[94] L. Feng, Z. Y. Zhang, Z. H. Mai, Y. M. Ma, B. Q. Liu, L. Jiang, D. B. Zhu, *Angew. Chem., Int. Ed.* **2004**, *43*, 2012.
[95] a) Z. L. Chu, Y. J. Feng, S. Seeger, *Angew. Chem., Int. Ed.* **2015**, *54*, 2328; b) R. K. Gupta, G. J. Dunderdale, M. W. England, A. Hozumi, *J. Mater. Chem. A* **2017**, *5*, 16025.
[96] a) D. K. Li, Z. G. Guo, *J. Colloid Interface Sci.* **2017**, *503*, 124; b) G. Y. Liu, W. Wang, D. Yu, *Cellulose* **2019**, *26*, 3529; c) K. L. Chen, J. L. Zhou, F. Q. Ge, R. Zhao, C. X. Wang, *Colloids Surf. A* **2019**, *565*, 86.
[97] Y. W. Huang, Y. X. Shan, S. Liang, X. L. Zhao, G. Jiang, C. Y. Hu, J. X. Yang, L. L. Liu, *J. Mater. Chem. A* **2018**, *6*, 17156.
[98] a) L. Yu, J. D. Ding, *Chem. Soc. Rev.* **2008**, *37*, 1473; b) N. A. Peppas, J. Z. Hilt, A. Khademhosseini, R. Langer, *Adv. Mater.* **2006**, *18*, 1345.
[99] L. Mi, S. Y. Jiang, *Angew. Chem., Int. Ed.* **2014**, *53*, 1746.
[100] Z. Wei, J. H. Yang, J. X. Zhou, F. Xu, M. Zrinyi, P. H. Dussault, Y. Osada, Y. M. Chen, *Chem. Soc. Rev.* **2014**, *43*, 8114.
[101] L. Li, B. Yan, J. Q. Yang, L. Y. Chen, H. B. Zeng, *Adv. Mater.* **2015**, *27*, 1294.
[102] W. D. Wang, L. Xiang, L. Gong, W. H. Hu, W. J. Huang, Y. J. Chen, A. B. Asha, S. Srinivas, L. Y. Chen, R. Narain, H. B. Zeng, *Chem. Mater.* **2019**, *31*, 2366.
[103] a) S. L. Banerjee, K. Bhattacharya, S. Samanta, N. K. Singha, *ACS Appl. Mater. Interfaces* **2018**, *10*, 27391; b) N. Y. Kostina, S. Sharifi, A. D. Pereira, J. Michalek, D. W. Grijpma, C. Rodriguez-Emmenegger, *J. Mater. Chem. B* **2013**, *1*, 5644; c) J. Z. Pan, Y. Jin, S. Q. Lai, L. J. Shi, W. H. Fan, Y. C. Shen, *Chem. Eng. J.* **2019**, *370*, 1228; d) L. Li, B. Yan, J. Q. Yang, W. J. Huang, L. Y. Chen, H. B. Zeng, *ACS Appl. Mater. Interfaces* **2017**, *9*, 9221; e) F. Wahid, Y. N. Zhou, H. S. Wang, T. Wan, C. Zhong, L. Q. Chu, *Int. J. Biol. Macromol.* **2018**, *114*, 1233.
[104] W. J. Yang, X. Tao, T. T. Zhao, L. X. Weng, E. T. Kang, L. H. Wang, *Polym. Chem.* **2015**, *6*, 7027.
[105] H. B. Wang, H. F. Li, Y. H. Wu, J. H. Yang, W. G. Liu, *Sci. China: Technol. Sci.* **2019**, *62*, 569.
[106] H. Chen, R. Y. Cheng, X. Zhao, Y. H. Zhang, A. Tam, Y. F. Yan, H. K. Shen, Y. S. Zhang, J. Qi, Y. Feng, L. Liu, G. Q. Pan, W. G. Cui, L. F. Deng, *NPG Asia Mater.* **2019**, *11*, 12.
[107] B. W. Li, P. Jain, J. R. Ma, J. K. Smith, Z. F. Yuan, H. C. Hung, Y. W. He, X. J. Lin, K. Wu, J. Pfaendtner, S. Y. Jiang, *Sci. Adv.* **2019**, *5*, 10.
[108] a) J. J. Koh, G. J. H. Lim, X. Zhou, X. W. Zhang, J. Ding, C. B. He, *ACS Appl. Mater. Interfaces* **2019**, *11*, 13787; b) Y. Yang, X. J. Li, X. Zheng, Z. Y. Chen, Q. F. Zhou, Y. Chen, *Adv. Mater.* **2018**, *30*, 11.